JHEP

Published for SISSA by Springer

Received: May 21, 2017
Revised: June 24, 2017
Accepted: July 17, 2017
Published: July 25, 2017

Predictive Pati-Salam theory of fermion masses and mixing

A. E. Cárcamo Hernández,[a] **Sergey Kovalenko,**[a] **José W.F. Valle**[b] **and C.A. Vaquera-Araujo**[b]

[a] *Universidad Técnica Federico Santa María and Centro Científico-Tecnológico de Valparaíso, Casilla 110-V, Valparaíso, Chile*

[b] *AHEP Group, Institut de Física Corpuscular — C.S.I.C./Universitat de València, Parc Científic de Paterna, C/Catedrático José Beltrán, 2 E-46980 Paterna, Valencia, Spain*

E-mail: antonio.carcamo@usm.cl, sergey.kovalenko@usm.cl, valle@ific.uv.es, vaquera@ific.uv.es

Abstract: We propose a Pati-Salam extension of the standard model incorporating a flavor symmetry based on the $\Delta(27)$ group. The theory realizes a realistic Froggatt-Nielsen picture of quark mixing and a predictive pattern of neutrino oscillations. We find that, for normal neutrino mass ordering, the atmospheric angle must lie in the higher octant, CP must be violated in oscillations, and there is a lower bound for the $0\nu\beta\beta$ decay rate. For the case of inverted mass ordering, we find that the lower atmospheric octant is preferred, and that CP can be conserved in oscillations. Neutrino masses arise from a low-scale seesaw mechanism, whose messengers can be produced by a Z' portal at the LHC.

Keywords: Beyond Standard Model, Neutrino Physics

ArXiv ePrint: 1705.06320

https://doi.org/10.1007/JHEP07(2017)118

JHEP07(2017)118

Contents

1 Introduction

Apart from the discovery of neutrino oscillations [1, 2], no other laboratory evidence for physics beyond the standard model has been so far unambiguously confirmed. Both the origin of neutrino mass itself, as well as the understanding of the mixing pattern, require an explanation from *first principles*. Moreover, there is a variety of other motivations for having beyond the standard model physics [3]. One of these is the pursuit of a dynamical explanation for the origin of parity violation in the weak interaction, whose basic V-A nature is put in by hand in the formulation of the standard model. With this in mind here we propose a flavored [4–6] Pati-Salam [7] extension of the standard model, addressing both the dynamical origin of the V-A nature of the weak force, as well as the related origin of neutrino mass. In addition, as we will see, the model can shed light upon the flavor problem and make predictions. The main features of our model include:

- adequate implementation of $\Delta(27)$ flavor symmetry in the Pati-Salam framework and symmetry breaking;
- consistent low-scale left-right symmetric seesaw mechanism for neutrinos [8–12];
- predictive pattern of neutrino mixing summarized in figures 1 and 2;
- realistic pattern of quark mixing, yielding a Froggatt-Nielsen [13]-like picture of the CKM matrix;
- lower bound for the $0\nu\beta\beta$ decay rate in figure 3.

JHEP07(2017)118

Field	$\overline{F}_{iL}$	F_{iR}	$\overline{\Psi}_{iL}$	Ψ_{iR}	S_i	χ_L	χ_R	Φ_j	Σ	ϕ_k	φ_l	σ	ρ_k	η_k	τ_k	ξ_k
$\mathrm{SU}(4)_C$	$\overline{\mathbf{4}}$	$\mathbf{4}$	$\overline{\mathbf{4}}$	$\mathbf{4}$	$\mathbf{1}$	$\mathbf{4}$	$\mathbf{4}$	$\mathbf{1}$	$\mathbf{15}$	$\mathbf{1}$	$\mathbf{1}$	$\mathbf{1}$	$\mathbf{1}$	$\mathbf{1}$	$\mathbf{1}$	$\mathbf{1}$
$SU(2)_L$	$\mathbf{2}$	$\mathbf{1}$	$\mathbf{1}$	$\mathbf{1}$	$\mathbf{1}$	$\mathbf{2}$	$\mathbf{1}$	$\mathbf{2}$	$\mathbf{1}$	$\mathbf{2}$	$\mathbf{1}$	$\mathbf{1}$	$\mathbf{1}$	$\mathbf{1}$	$\mathbf{1}$	$\mathbf{1}$
$SU(2)_R$	$\mathbf{1}$	$\mathbf{2}$	$\mathbf{1}$	$\mathbf{1}$	$\mathbf{1}$	$\mathbf{1}$	$\mathbf{2}$	$\mathbf{2}$	$\mathbf{1}$	$\mathbf{1}$	$\mathbf{2}$	$\mathbf{1}$	$\mathbf{1}$	$\mathbf{1}$	$\mathbf{1}$	$\mathbf{1}$

Table 1. Particle content and transformation properties under the gauge symmetry.

We note also that the model has a low-scale Z' portal through which the TeV scale messengers S_a can be pair-produced in Drell-Yan collisions at the LHC [14–16]. In addition, our model realizes a universal seesaw mechanism [17] for the down type quarks as well as the charged leptons, mediated by TeV scale exotic fermions. The latter should potentially lead to other phenomenological effects in the quark sector as well as lepton flavour violation effects.

2 The model

The model under consideration is based on the Pati-Salam gauge symmetry $\mathrm{SU}(4)_C \otimes SU(2)_L \otimes SU(2)_R$, supplemented by the $\Delta(27) \otimes Z_4 \otimes Z_{16}$ discrete family symmetry group. The fermion transformation properties under the Pati-Salam group are

$$\begin{aligned} &\overline{F}_{iL} \sim \left(\overline{\mathbf{4}}, \mathbf{2}, \mathbf{1}\right), && F_{iR} \sim (\mathbf{4}, \mathbf{1}, \mathbf{2}), && S_i \sim (\mathbf{1}, \mathbf{1}, \mathbf{1}), \\ &\overline{\Psi}_{iL} \sim \left(\overline{\mathbf{4}}, \mathbf{1}, \mathbf{1}\right), && \Psi_{iR} \sim (\mathbf{4}, \mathbf{1}, \mathbf{1}), && i = 1, 2, 3, \end{aligned} \tag{2.1}$$

where the subscript refers to fermion families. More explicitly, the standard model fermions are written in component form as

$$\overline{F}_{iL} = \begin{pmatrix} \overline{u}_{iL} & \overline{u}_{iL} & \overline{u}_{iL} & \overline{\nu}_{iL} \\ \overline{d}_{iL} & \overline{d}_{iL} & \overline{d}_{iL} & \overline{l}_{iL} \end{pmatrix}^T, \qquad F_{iR} = \begin{pmatrix} u_{iR} & u_{iR} & u_{iR} & \nu_{iR} \\ d_{iR} & d_{iR} & d_{iR} & l_{iR} \end{pmatrix}. \tag{2.2}$$

Notice that we have extended the fermion sector of the original Pati-Salam model [7] by introducing three fermion singlets S_i, in order to implement inverse and/or linear seesaw mechanisms for the generation of light active neutrino masses [8–12]. In addition, we have introduced vector-like fermions $\overline{\Psi}_{iL}$ and Ψ_{iR} so as to generate the standard model down-type quark and charged lepton masses, from a universal seesaw mechanism.

The particle content and gauge symmetry assignments are summarized in table 1.

The fermion assignments under the flavor symmetry group $\Delta(27) \otimes Z_4 \otimes Z_{16}$ are:

$$\begin{aligned} &\overline{F}_{1L} \sim (\mathbf{1_{0,0}}, 1, i), && \overline{F}_{2L} \sim \left(\mathbf{1_{2,0}}, i, i^{\frac{1}{2}}\right), && \overline{F}_{3L} \sim (\mathbf{1_{1,0}}, 1, 1), \\ &F_{1R} \sim (\mathbf{1_{0,0}}, 1, i), && F_{2R} \sim \left(\mathbf{1_{1,0}}, i, i^{\frac{1}{2}}\right), && F_{3R} \sim (\mathbf{1_{2,0}}, 1, 1), \\ &\overline{\Psi}_{1L} \sim (\mathbf{1_{0,0}}, 1, 1) && \overline{\Psi}_{2L} \sim (\mathbf{1_{2,0}}, 1, 1), && \overline{\Psi}_{3L} \sim (\mathbf{1_{1,0}}, 1, 1) \\ &\Psi_{1R} \sim (\mathbf{1_{0,0}}, 1, 1), && \Psi_{2R} \sim (\mathbf{1_{1,0}}, 1, 1), && \Psi_{3R} \sim (\mathbf{1_{2,0}}, 1, 1), \\ & && S \sim (\mathbf{3}, i, 1), \end{aligned} \tag{2.3}$$

JHEP07(2017)118

Field	$\overline{F}_{1L}$	$\overline{F}_{2L}$	$\overline{F}_{3L}$	F_{1R}	F_{2R}	F_{3R}	$\overline{\Psi}_{1L}$	$\overline{\Psi}_{2L}$	$\overline{\Psi}_{3L}$	Ψ_{1R}	Ψ_{2R}	Ψ_{3R}	S
$\Delta(27)$	$\mathbf{1_{0,0}}$	$\mathbf{1_{2,0}}$	$\mathbf{1_{1,0}}$	$\mathbf{1_{0,0}}$	$\mathbf{1_{1,0}}$	$\mathbf{1_{2,0}}$	$\mathbf{1_{0,0}}$	$\mathbf{1_{2,0}}$	$\mathbf{1_{1,0}}$	$\mathbf{1_{0,0}}$	$\mathbf{1_{1,0}}$	$\mathbf{1_{2,0}}$	$\mathbf{3}$
Z_4	1	i	1	1	i	1	1	1	1	1	1	1	i
Z_{16}	i	$i^{\frac{1}{2}}$	1	i	$i^{\frac{1}{2}}$	1	1	1	1	1	1	1	1

Table 2. Transformation properties of the leptons and quarks under the flavor symmetry $\Delta(27) \otimes Z_4 \otimes Z_4'$.

where the numbers in boldface stand for the dimensions of the $\Delta\,(27)$ irreducible representations, and we have defined $S \equiv (S_1, S_2, S_3)$. Notice that the three Pati-Salam singlet fermions are grouped into a $\Delta\,(27)$ triplet S, whereas the remaining fermions are assigned to singlet representations of $\Delta\,(27)$. These fermion flavor symmetry transformation properties are summarized in table 2. A brief summary of the properties of $\Delta\,(27)$ group and its irreducible representations is given in appendix A.

We now turn to the main features of the scalar sector. The Higgs fields of the model are assumed to transform under the Pati-Salam gauge group as

$$\begin{aligned}
&\chi_R \sim (\mathbf{4},\mathbf{1},\mathbf{2})\,, \quad \chi_L \sim (\mathbf{4},\mathbf{2},\mathbf{1})\,, \quad \Phi_j \sim (\mathbf{1},\mathbf{2},\mathbf{2})\,, \quad \Sigma \sim (\mathbf{15},\mathbf{1},\mathbf{1})\,, \quad j=1,2,\\
&\phi_k \sim (\mathbf{1},\mathbf{2},\mathbf{1})\,, \quad \varphi_l \sim (\mathbf{1},\mathbf{1},\mathbf{2})\,, \quad \sigma \sim (\mathbf{1},\mathbf{1},\mathbf{1})\,, \quad \rho_k \sim (\mathbf{1},\mathbf{1},\mathbf{1})\,, \quad l=1,2,3,4,5,\\
&\eta_k \sim (\mathbf{1},\mathbf{1},\mathbf{1})\,, \quad \tau_k \sim (\mathbf{1},\mathbf{1},\mathbf{1})\,, \quad \xi_k \sim (\mathbf{1},\mathbf{1},\mathbf{1})\,, \qquad\qquad k=1,2,3, \qquad (2.4)
\end{aligned}$$

and the scalars $\chi_{L,R}$, Φ_k and Σ develop vacuum expectation values (VEVs) of the form

$$\langle \chi_{L,R} \rangle = \begin{pmatrix} 0 & 0 & 0 & v_{L,R} \\ 0 & 0 & 0 & 0 \end{pmatrix}, \qquad \langle \Phi_j \rangle = \begin{pmatrix} v_1^{(j)} & 0 \\ 0 & v_2^{(j)} \end{pmatrix}, \qquad \langle \Sigma \rangle = v_\Sigma T^{15}, \qquad (2.5)$$

with $T^{15} = \frac{1}{2\sqrt{6}}\mathrm{diag}\,(1,1,1,-3)$.

The transformation properties of the scalar fields under the $\Delta\,(27) \otimes Z_4 \otimes Z_{16}$ discrete group are given as follows:

$$\begin{aligned}
&\chi_R \sim (\mathbf{1_{0,0}}, i, 1)\,, && \chi_L \sim (\mathbf{1_{0,0}}, -i, 1)\,, && \Phi_1 \sim (\mathbf{1_{0,0}}, 1, 1)\,, && \Phi_2 \sim (\mathbf{1_{0,0}}, -1, 1)\,,\\
&\Sigma \sim \left(\mathbf{1_{0,0}}, 1, e^{\frac{3\pi i}{4}}\right), && \phi_1 \sim \left(\mathbf{1_{0,0}}, 1, e^{-\frac{2\pi i}{8}}\right), && \phi_2 \sim \left(\mathbf{1_{0,0}}, -i, e^{-\frac{\pi i}{8}}\right), && \phi_3 \sim (\mathbf{1_{0,0}}, 1, 1)\,,\\
&\varphi_1 \sim \left(\mathbf{1_{0,0}}, 1, e^{-\frac{2\pi i}{8}}\right), && \varphi_2 \sim \left(\mathbf{1_{0,0}}, -i, e^{-\frac{\pi i}{8}}\right), && \varphi_3 \sim (\mathbf{1_{0,0}}, 1, 1)\,, && \varphi_4 \sim \left(\mathbf{1_{2,0}}, -i, e^{-\frac{\pi i}{8}}\right),\\
&\varphi_5 \sim \left(\mathbf{1_{2,0}}, 1, e^{\frac{\pi i}{8}}\right), && \sigma \sim \left(\mathbf{1_{0,0}}, 1, e^{-\frac{\pi i}{8}}\right), && \rho \sim (\overline{\mathbf{3}}, 1, i) && \eta \sim \left(\overline{\mathbf{3}}, -i, i^{\frac{1}{2}}\right),\\
& && \tau \sim (\overline{\mathbf{3}}, 1, 1)\,, && \xi \sim (\overline{\mathbf{3}}, -1, 1) &&
\end{aligned} \qquad (2.6)$$

where we have set

$$\rho \equiv (\rho_1, \rho_2, \rho_3) \qquad \eta = (\eta_1, \eta_2, \eta_3) \qquad \tau \equiv (\tau_1, \tau_2, \tau_3) \qquad \xi \equiv (\xi_1, \xi_2, \xi_3)\,. \qquad (2.7)$$

These flavor symmetry scalar transformation properties are summarized in table 3.

JHEP07(2017)118

Field	χ_L	χ_R	Φ_1	Φ_2	Σ	ϕ_1	ϕ_2	ϕ_3	φ_1	φ_2	φ_3	φ_4	φ_5	σ	ρ	η	τ	ξ
$\Delta(27)$	$\mathbf{1_{0,0}}$	$\mathbf{1_{0,0}}$	$\mathbf{1_{0,0}}$	$\mathbf{1_{0,0}}$	$\mathbf{1_{0,0}}$	$\mathbf{1_{0,0}}$	$\mathbf{1_{0,0}}$	$\mathbf{1_{0,0}}$	$\mathbf{1_{0,0}}$	$\mathbf{1_{0,0}}$	$\mathbf{1_{0,0}}$	$\mathbf{1_{2,0}}$	$\mathbf{1_{2,0}}$	$\mathbf{1_{0,0}}$	$\overline{\mathbf{3}}$	$\overline{\mathbf{3}}$	$\overline{\mathbf{3}}$	$\overline{\mathbf{3}}$
Z_4	$-i$	i	1	-1	1	1	$-i$	1	1	$-i$	1	$-i$	1	1	1	$-i$	1	-1
Z_{16}	1	1	1	1	$i^{\frac{3}{2}}$	$i^{-\frac{1}{2}}$	$i^{-\frac{1}{4}}$	1	$i^{-\frac{1}{2}}$	$i^{-\frac{1}{4}}$	1	$i^{-\frac{1}{4}}$	$i^{\frac{1}{4}}$	$i^{-\frac{1}{4}}$	i	$i^{\frac{1}{2}}$	1	1

Table 3. Transformation properties of the scalars under the flavor symmetry $\Delta(27) \otimes Z_4 \otimes Z_4'$.

With the above particle content and transformation properties the following relevant Yukawa terms arise:

$$
\begin{aligned}
-\mathcal{L}_Y = {} & y_1 \overline{F}_{1L} \Phi_1 F_{1R} \frac{\sigma^8}{\Lambda^8} + y_2 \overline{F}_{2L} \Phi_2 F_{2R} \frac{\sigma^4}{\Lambda^4} + y_3 \overline{F}_{3L} \Phi_1 F_{3R} \\
& + \frac{\alpha_1}{\Lambda} \overline{F}_{1L} \chi_L \left(S\rho\right)_{\mathbf{1_{0,0}}} \frac{\sigma^8}{\Lambda^8} + \frac{\alpha_2}{\Lambda} \overline{F}_{2L} \chi_L \left(S\eta\right)_{\mathbf{1_{1,0}}} \frac{\sigma^4}{\Lambda^4} + \frac{\alpha_3}{\Lambda} \overline{F}_{3L} \chi_L \left(S\tau\right)_{\mathbf{1_{2,0}}} \\
& + \frac{\beta_1}{\Lambda} F_{1R} \chi_R^{\dagger} \left(S\rho\right)_{\mathbf{1_{0,0}}} \frac{\sigma^8}{\Lambda^8} + \frac{\beta_2}{\Lambda} F_{2R} \chi_R^{\dagger} \left(S\eta\right)_{\mathbf{1_{2,0}}} \frac{\sigma^4}{\Lambda^4} + \frac{\beta_3}{\Lambda} F_{3R} \chi_R^{\dagger} \left(S\tau\right)_{\mathbf{1_{1,0}}} \\
& + \kappa_1 \overline{F}_{1L} \phi_1 \Psi_{1R} \frac{\sigma^2}{\Lambda^2} + \kappa_2 \overline{F}_{2L} \phi_2 \Psi_{2R} \frac{\sigma}{\Lambda} + \kappa_3 \overline{F}_{3L} \phi_3 \Psi_{3R} \\
& + \gamma_1 \overline{\Psi}_{1L} \varphi_1 F_{1R} \frac{\sigma^2}{\Lambda^2} + \gamma_2 \overline{\Psi}_{2L} \varphi_2 F_{2R} \frac{\sigma}{\Lambda} + \gamma_3 \overline{\Psi}_{3L} \varphi_3 F_{3R} \\
& + \gamma_4 \overline{\Psi}_{1L} \varphi_4 F_{2R} \frac{\sigma}{\Lambda} + \gamma_5 \overline{\Psi}_{1L} \varphi_5^* F_{3R} \frac{\sigma^*}{\Lambda} + \gamma_6 \overline{\Psi}_{2L} \varphi_5 F_{3R} \frac{\sigma}{\Lambda} \\
& + \sum_{i=1}^{3} \left[A_i \overline{\Psi}_{iL} \Psi_{iR} + a_i \overline{\Psi}_{riL} \left(\Sigma\right)_s^r \Psi_{iR}^s \frac{\sigma^6}{\Lambda^6} \right] + \lambda_1 \left(\overline{S} S^C\right)_{\mathbf{3}_{S_1}} \xi + \lambda_2 \left(\overline{S} S^C\right)_{\mathbf{3}_{S_2}} \xi + \text{h.c.},
\end{aligned}
\tag{2.8}
$$

where r, s are $SU\left(4\right)$ indices and y_i, α_i, β_i, κ_i, a_i $(i = 1, 2, 3)$, γ_m $(m = 1, 2, \cdots, 6)$ and λ_j $(j = 1, 2)$ are $\mathcal{O}(1)$ dimensionless couplings. For an explanation of the $\Delta(27)$ notation used in the α, β and λ-terms, see appendix A. It is noteworthy that the lightest of the physical neutral scalar states of $\left(\Phi_j\right)_{11}$, $\left(\Phi_j\right)_{22}$, ϕ_i should be interpreted as the SM-like 125 GeV Higgs recently found at the LHC. Furthermore, our model at low energies corresponds to a seven Higgs doublet model with five scalar singlets (these scalar singlets come from φ_l). As we will show in section 4, the top quark mass only arises from $\left(\Phi_1\right)_{11}$. Consequently, the dominant contribution to the SM-like 125 GeV Higgs mainly arises from $\left(\Phi_1\right)_{11}$. We note also that the scalar potential of our model has many free parameters, so that we can assume the remaining scalars to be heavy and outside the LHC reach. Moreover, one can suppress the loop effects of the heavy scalars contributing to precision observables, by making an appropriate choice of the free parameters in the scalar potential. These adjustments do not affect the physical observables in the quark and lepton sectors, which are determined mainly by the Yukawa couplings.

The full symmetry group $\mathcal{G}$ exhibits the following spontaneous breaking pattern:

$$
\begin{gathered}
\mathcal{G} = \mathrm{SU}(4)_C \otimes SU\left(2\right)_L \otimes SU\left(2\right)_R \otimes \Delta\left(27\right) \otimes Z_4 \otimes Z_{16} \\
\langle \Sigma \rangle \sim \Lambda_{PS} \\
\Downarrow
\end{gathered}
\tag{2.9}
$$

$$\mathrm{SU}(3)_C \otimes SU\,(2)_L \otimes SU\,(2)_R \otimes U\,(1)_{B-L} \tag{2.10}$$

$$\langle \chi_R \rangle \sim \ v_R$$

$$\Downarrow$$

$$\mathrm{SU}(3)_C \otimes SU\,(2)_L \otimes U\,(1)_Y \tag{2.11}$$

$$\langle \Phi_{1,2} \rangle \sim \ v$$

$$\Downarrow$$

$$\mathrm{SU}(3)_C \otimes U\,(1)_Q\,. \tag{2.12}$$

Here $v = 246\,\mathrm{GeV}$ is the electroweak symmetry breaking scale, and we assume that the Pati-Salam gauge symmetry is broken at the scale $\Lambda_{PS} \gtrapprox 10^6\,\mathrm{GeV}$. This restriction follows from the experimental limit on the branching ratio for the rare neutral meson decays, such as $B^0 \to l_i^{\pm} l_j^{\mp}$, mediated by the vector leptoquarks, as discussed in refs. [18, 19]. Furthermore, it is worth mentioning that Pati-Salam models with a quark-lepton unification scale of about $\gtrapprox 10^6\,\mathrm{GeV}$ can fulfill gauge coupling unification [20]. A comprehensive study of gauge coupling unification in models that include all possible chains of Pati-Salam symmetry breaking in both supersymmetric and non-supersymmetric scenarios has been given in ref. [20].

3 Understanding the model setup

In this section we try to motivate in more detail our choice for the model content and the transformation properties. First note that the Pati-Salam gauge symmetry $\mathrm{SU}(4)_C \otimes SU\,(2)_L \otimes SU\,(2)_R$ breaks down to the conventional left-right symmetry $\mathrm{SU}(3)_C \otimes SU\,(2)_L \otimes SU\,(2)_R \otimes U\,(1)_{B-L}$ by the VEV of the scalar field Σ, at the scale $\Lambda_{PS} \gtrapprox 10^6\,\mathrm{GeV}$. The next symmetry breaking step is triggered by χ_R, whose VEV is assumed to be in the few TeV scale, playing an important role in implementing the low-scale seesaw neutrino mass generation [9, 10]. The breaking of the electroweak gauge group $\mathrm{SU}(3)_C \otimes SU\,(2)_L \otimes U\,(1)_Y$ is triggered by the scalar fields Φ_j, which acquire vacuum expectation values at the electroweak symmetry breaking scale $v = 246\,\mathrm{GeV}$.

Besides, note that the presence of the scalar field Σ transforming as the adjoint representation of $SU\,(4)$ is also crucial in the implementation of the Universal Seesaw mechanism for down-type quarks and charged leptons, mediated by exotic fermions. This scalar field Σ acquires a VEV at the scale Λ_{PS}, so that an insertion $\frac{\sigma^6}{\Lambda^6}$ in its corresponding Yukawa term generates a TeV scale contribution to the exotic charged lepton and exotic down-type quark masses. The charge of Σ under the Z_{16} discrete group ensures that its different contributions to the charged leptons and down type quark masses will be comparable to the ones arising from the $A_i \overline{\Psi}_{iL} \Psi_{iR}$ $(i = 1, 2, 3)$ mass terms (which contribute equally to the down type quark and charged lepton masses). It is worth mentioning that we are assuming $A_i \approx \mathcal{O}(1)\,\mathrm{TeV}$. Let us note that the inclusion of the scalar field Σ is necessary to guarantee that the resulting down-type quark masses are different from the charged lepton masses, as it will be shown in section 4.

JHEP07(2017)118

Notice that the scalars ϕ_i and φ_l are needed to generate the mixing between the standard model charged leptons and down-type quarks with their exotic siblings, so as to implement the Universal Seesaw mechanism that gives rise to realistic masses for the standard model charged fermions. The scalar fields χ_R, χ_L and ξ_i have Yukawa terms necessary for the implementation of the inverse and linear seesaw mechanisms, so as to generate the light active neutrino masses. This requires also that VEVs of ξ_i are much smaller than the electroweak symmetry breaking scale.

The scalar fields ρ_i , η_i and τ_i are needed to generate the diagonal 3×3 blocks that include the mixing of the neutrino states contained in $\overline{F}_{iL}$ and F_{iR} with the singlet neutrinos S_i $(i = 1, 2, 3)$, thus avoiding the transmission of the strong hierarchy in the up mass matrix to the light active neutrino mass matrix. Furthermore, the scalar field σ, charged under the Z_{16} discrete group is need to generate the observed SM charged fermion mass and quark mixing hierarchy. In order to relate the quark masses with the quark mixing parameters, we assume that the scalar field σ acquires a VEV equal to $\lambda\Lambda$, where $\lambda = 0.225$ is one of the Wolfenstein parameters and Λ is the cutoff of our model. In summary, the set of VEVs of the scalar fields is assumed to satisfy the following hierarchy:

$$v_L \ll v_\xi \ll v_1^{(j)} \sim v_{\phi_i} \sim v_{\varphi_l} \sim v \ll v_R \ll v_\rho = v_\eta = v_\tau \sim \Lambda_{PS} \sim v_\sigma = \lambda\Lambda, \tag{3.1}$$

where $\langle \chi_{L,R} \rangle = v_{L,R}$. We now comment on the possible VEV patterns for the $\Delta(27)$ scalar triplets ρ, η, τ and ξ. Since the VEVs of the $\Delta(27)$ scalar triplets satisfy the hierarchy $v_\xi \ll v_\rho = v_\eta = v_\tau \sim \Lambda_{PS}$, the mixing angles of ξ with ρ, η and τ are very tiny since they are suppressed by the ratios of their VEVs, and consequently the method of recursive expansion proposed in ref. [21] can be used for the analysis of the model scalar potential. In this scenario, the scalar potential for the $\Delta(27)$ scalar triplet ξ can be treated independently from the scalar potential for the $\Delta(27)$ scalar triplets ρ, η, τ, as shown in detail in the appendices B and C. One can see that the following VEV patterns for the $\Delta(27)$ scalar triplets are consistent with the scalar potential minimization equations for a large region of parameter space

$$\begin{aligned} &\langle \rho \rangle = v_\rho \, (1, 0, 0) \, , \qquad \langle \eta \rangle = v_\eta \, (0, 1, 0) \, , \qquad \langle \tau \rangle = v_\tau \, (0, 0, 1) \, , \\ &\langle \xi \rangle = \frac{v_\xi}{\sqrt{2 + r^2}} \left(r, e^{-i\psi}, e^{i\psi} \right) . \end{aligned} \tag{3.2}$$

We now turn our attention on the role of each discrete group factor of our model. As will be seen in sections 4 and 5 the $\Delta\,(27)$ discrete group is crucial for the predictivity of our model, giving rise to viable textures for the fermion masses and mixings. Notice that the $\Delta(27)$ discrete group is a non trivial group of the type $\Delta(3n^2)$ for $n = 3$, isomorphic to the semi-direct product group $(Z_3' \times Z_3'') \rtimes Z_3$ [4]. Recently, this group has been used in multi-Higgs doublet models [22], SO(10) models [23], warped extra dimensional models [24] and models based on the $\mathrm{SU}(3)_C \otimes \mathrm{SU}(3)_L \otimes \mathrm{U}(1)_X$ gauge symmetry [25, 26]. We introduce the Z_{16} discrete group, since it is the smallest cyclic symmetry that allows the Yukawa term $\overline{F}_{1L}\Phi_1 F_{1R}\frac{\sigma^8}{\Lambda^8}$ of dimension twelve from a $\frac{\sigma^8}{\Lambda^8}$ insertion on the $\overline{F}_{1L}\Phi_1 F_{1R}$ operator. This leads to the required λ^8 suppression needed to naturally explain the smallness of

JHEP07(2017)118

the up quark mass. The Z_{16} group has been recently shown to be useful for explaining the observed SM charged fermion mass and quark mixing hierarchy, in the framework of a $\mathrm{SU}(3)_C \otimes \mathrm{SU}(3)_L \otimes \mathrm{U}(1)_X$ models based on the A_4 and S_3 family symmetries [27–29]. As we will see in the next section, in our model the CKM matrix arises from the down-type quark sector. In order to get the correct hierarchy in the entries of the quark mass matrices yielding a realistic pattern of quark masses and mixing angles, we use a Z_4 discrete symmetry and the scalar bidoublets Φ_j $(j = 1, 2)$, one neutral and the another charged under Z_4. This group was previously used in some other flavor models and proved to be helpful, in particular, in the context of Grand Unification [30, 31], models with extended $\mathrm{SU}(3)_C \otimes \mathrm{SU}(3)_L \otimes \mathrm{U}(1)_X$ gauge symmetry [32] and warped extradimensional models [33]. The Z_4 is the smallest cyclic symmetry that guarantees that the renormalizable Yukawa terms for the fermion singlets S_i $(i = 1, 2, 3)$ only involve the scalar fields ξ_i, assumed to acquire very small VEVs. This feature is crucial to obtain an inverse seesaw contribution to the light active neutrino mass matrix, instead of a double seesaw contribution, thus giving rise to heavy quasi-Dirac neutrinos within the LHC reach.

It is worth noting that the Yukawa Lagrangian (2.8) possesses accidental U_1-symmetries located in the non-SM sector with the field charge (Q) assignments:

$$U_1^{(a)}: \quad Q^{(a)}(S) = 1, \qquad Q^{(a)}(\xi) = Q^{(a)}(\zeta) = 2, \qquad Q^{(a)}(\rho) = Q^{(a)}(\eta) = Q^{(a)}(\tau) = -1. \tag{3.3}$$

$$U_1^{(b)}: \quad Q^{(b)}(S) = 1, \qquad Q^{(b)}(\xi) = Q^{(b)}(\zeta) = 2, \qquad Q^{(b)}(\chi_L) = -Q^{(b)}(\chi_R) = -1. \tag{3.4}$$

These are spontaneously broken by the VEVs of the corresponding scalar fields in eq. (3.2). As a result there appear massless Goldstone bosons with interaction strengths determined by the VEVs shown in eq. (3.2). This leads to the presence of invisible Higgs decays [34] which are restricted by LEP as well as LHC searches [35]. From eq. (3.1) one sees that the $U_1^{(a)}$ symmetry breaking scale is large of the order of $\Lambda_{PS} \sim 10^6\,\mathrm{GeV}$, while the $U_1^{(b)}$ symmetry is broken at the low scale $v_\xi \sim v_\zeta$. Thus the $U_1^{(b)}$-Goldstone can have a significant couplings with the fields in the exotic sector and these interactions could potentially leak via mixing to the SM sector. On the other hand, as previously mentioned in section 2, the 125 GeV Higgs boson is dominantly composed of $(\Phi_1)_{11}$, which is the only scalar contributing to the top quark mass. Since the $U_1^{(b)}$ symmetry breaking scale $v_\xi \sim v_\zeta$ is much smaller than the scale of electroweak symmetry breaking scale $v = 246\,\mathrm{GeV}$, the mixing of the $U_1^{(b)}$-Goldstone with the 125 GeV Higgs boson is suppressed by the ratios of their VEVs (cf. ref. [21]). Alternatively, these Goldstones may also be avoided by adding explicit breaking trilinear terms in the scalar potential. A detailed study is beyond the scope of the present paper.

4 Quark masses and mixings

From the first line in eq. (2.8), the up-type quark mass matrix is given by

$$M_U = \begin{pmatrix} y_1\lambda^8 & 0 & 0 \\ 0 & y_2\lambda^4 & 0 \\ 0 & 0 & y_3 \end{pmatrix} \frac{v}{\sqrt{2}}, \tag{4.1}$$

JHEP07(2017)118

where y_i $(i = 1, 2, 3)$ are $\mathcal{O}(1)$ parameters and we set $v_1^{(1)} = v_1^{(2)} = \frac{v}{\sqrt{2}}$, with $v = 246\,\text{GeV}$ the scale of electroweak symmetry breaking and $v_\sigma = \lambda\Lambda$, with $\lambda = 0.225$ being one of the Wolfenstein parameters.

For the sake of simplicity, we assume $v_2^{(j)} = 0$ $(j = 1, 2)$ so that the standard model down-type quarks and charged leptons acquire their masses from a universal seesaw mechanism, mediated by the exotic down-type quarks D_i and charged leptons L_i present in Ψ_{iR} and $\overline{\Psi}_{iL}$. In this case the down-type charged fermion mass matrices take the form

$$\left(\overline{d}_{iL}\ \overline{D}_{iL}\right)\begin{pmatrix} 0_{3\times3} & M_a \\ M_b & M_D \end{pmatrix}\begin{pmatrix} d_{jR} \\ D_{jR} \end{pmatrix}, \qquad \left(\overline{l}_{iL}\ \overline{L}_{iL}\right)\begin{pmatrix} 0_{3\times3} & M_a \\ M_b & M_l \end{pmatrix}\begin{pmatrix} l_{jR} \\ L_{jR} \end{pmatrix}, \tag{4.2}$$

with

$$\begin{aligned}
M_a &= \begin{pmatrix} \kappa_1\lambda^2 & 0 & 0 \\ 0 & \kappa_2\lambda & 0 \\ 0 & 0 & \kappa_3 \end{pmatrix} v_\phi\,, \qquad M_b = \begin{pmatrix} \gamma_1\lambda^2 & \gamma_4\lambda & \gamma_5\lambda \\ 0 & \gamma_2\lambda & \gamma_6\lambda \\ 0 & 0 & \gamma_3 \end{pmatrix} v_\varphi\,, \\
M_D &= \begin{pmatrix} A_1 + \frac{v_{\Sigma_2}}{2\sqrt{6}}a_1 & 0 & 0 \\ 0 & A_2 + \frac{v_{\Sigma_2}}{2\sqrt{6}}a_2 & 0 \\ 0 & 0 & A_3 + \frac{v_{\Sigma_2}}{2\sqrt{6}}a_3 \end{pmatrix}, \\
M_l &= \begin{pmatrix} A_1 - \frac{3v_{\Sigma_2}}{2\sqrt{6}}a_1 & 0 & 0 \\ 0 & A_2 - \frac{3v_{\Sigma_2}}{2\sqrt{6}}a_2 & 0 \\ 0 & 0 & A_3 - \frac{3v_{\Sigma_2}}{2\sqrt{6}}a_3 \end{pmatrix},
\end{aligned} \tag{4.3}$$

and the further simplification $v_{\phi_i} = v_\phi$ and $v_{\varphi_l} = v_\varphi$.

Taking the limit M_a, $M_b \ll A_i$, the standard model down-type quark and charged lepton mass matrices become

$$M_f^{(1)} = M_a\,(M_f)^{-1}\,M_b = \begin{pmatrix} a_{1f}\lambda^7 & a_{4f}\lambda^6 & a_{5f}\lambda^6 \\ 0 & a_{2f}\lambda^5 & a_{6f}\lambda^5 \\ 0 & 0 & a_{3f}\lambda^3 \end{pmatrix}\frac{v}{\sqrt{2}}, \qquad f = D, l. \tag{4.4}$$

where we have set $v_\phi = \lambda^3\frac{v}{\sqrt{2}}\frac{m_\Psi}{v_\varphi}$.

Notice that in our model the CKM matrix arises only from the down-type quark sector. In order to recover the low energy quark flavor data, we assume that all dimensionless parameters of the SM down-type quark mass matrix are real, excepting a_{5D}, taken to be complex. The physical quark mass spectrum [36, 37] and mixing angles [38] can be perfectly reproduced in terms of natural parameters of order one, as shown in table 4, starting from the following benchmark point:

$$\begin{aligned}
&y_1 \simeq 1.269\,, && y_2 \simeq 1.424\,, && y_3 \simeq 0.989\,, && \\
&a_{1D} \simeq 0.585\,, && a_{2D} \simeq 0.560\,, && a_{3D} \simeq 1.421\,, && \\
&a_{4D} \simeq 0.573\,, && |a_{5D}| \simeq 0.446\,, && \arg(a_{5D}) \simeq -1.906\,, && a_{6D} \simeq 1.153\,.
\end{aligned} \tag{4.5}$$

JHEP07(2017)118

Observable	Model value	Experimental value
m_u(MeV)	1.45	$1.45^{+0.56}_{-0.45}$
m_c(MeV)	635	635 ± 86
m_t(GeV)	172	$172.1 \pm 0.6 \pm 0.9$
m_d(MeV)	2.9	$2.9^{+0.5}_{-0.4}$
m_s(MeV)	57.7	$57.7^{+16.8}_{-15.7}$
m_b(GeV)	2.82	$2.82^{+0.09}_{-0.04}$
$\sin\theta_{12}$	0.225	0.225
$\sin\theta_{23}$	0.0411	0.0411
$\sin\theta_{13}$	0.00357	0.00357
δ	1.236	1.236

Table 4. Model and experimental values of the quark masses and CKM parameters.

To close this section we briefly comment on the phenomenological implications of our model regarding flavor changing processes involving quarks. It is noteworthy that the flavor changing top quark decays $t \to hc$ and $t \to hu$ are absent at tree level in our model, as follows from the quark Yukawa terms. The flavor changing top quark decays $t \to hc$ and $t \to hu$ are induced at one loop level from virtual charged Higgses and SM down-type quarks running in the internal lines of the loops. Consequently, a measurement of the branching fraction for the $t \to hc$ and $t \to hu$ decays at the LHC may test our model. On the other hand the admixture of exotic down-type quarks in the mass matrix implies a violation of the Glashow-Iliopoulos-Maiani mechanism in this sector. This may be relevant in connection with the recent B anomalies [39].

5 Lepton masses, mixing and oscillations

Here is where the predictive power of our flavor symmetry model is mainly manifest. From the neutrino Yukawa terms, we obtain the following neutrino mass terms:

$$-\mathcal{L}^{(\nu)}_{\text{mass}} = \frac{1}{2}\left(\overline{\nu_L^C}\ \overline{\nu_R}\ \overline{S}\right) M_\nu \begin{pmatrix} \nu_L \\ \nu_R^C \\ S^C \end{pmatrix} + \text{H.c.}, \tag{5.1}$$

where the neutrino mass matrix reads

$$\begin{aligned} M_\nu &= \begin{pmatrix} 0_{3\times3} & M_1 & M_2 \\ M_1^T & 0_{3\times3} & M_3 \\ M_2^T & M_3^T & \mu \end{pmatrix} = \begin{pmatrix} 0_{3\times3} & M_U & \frac{\sqrt{2}v_L v_\rho}{\Lambda v} M_U \\ M_U^T & 0_{3\times3} & \frac{\sqrt{2}v_R v_\rho}{\Lambda v} M_U \\ \frac{\sqrt{2}v_L v_\rho}{\Lambda v} M_U^T & \frac{\sqrt{2}v_R v_\rho}{\Lambda v} M_U^T & \mu \end{pmatrix} \\ &= \begin{pmatrix} 0_{3\times3} & M_U & \frac{v_L}{v_R} M_U \\ M_U^T & 0_{3\times3} & M_U \\ \frac{v_L}{v_R} M_U^T & M_U^T & \mu \end{pmatrix}, \end{aligned} \tag{5.2}$$

with

$$\mu = \begin{pmatrix} r\lambda_1 & \lambda_2 e^{i\psi} & \lambda_2 e^{-i\psi} \\ \lambda_2 e^{i\psi} & \lambda_1 e^{-i\psi} & r\lambda_2 \\ \lambda_2 e^{-i\psi} & r\lambda_2 & \lambda_1 e^{i\psi} \end{pmatrix} \frac{v_\xi}{\sqrt{2+r^2}}\,, \tag{5.3}$$

where for the sake of simplicity, we set $\alpha_i = \beta_i = y_i$ $(i = 1, 2, 3)$ and $v_\rho = v_\eta = v_\tau = \frac{v}{\sqrt{2}v_R}\Lambda$. Then,

$$\begin{aligned} M_\nu^{(1)} &= \mu - \frac{v_L}{v_R}\left(M_U + M_U^T\right), & M_\nu^{(2)} &= -\frac{1}{2}\left(M_U + M_U^T\right) + \frac{1}{2}\mu, \\ M_\nu^{(3)} &= \frac{1}{2}\left(M_U + M_U^T\right) + \frac{1}{2}\mu \end{aligned} \tag{5.4}$$

where $M_\nu^{(1)}$ corresponds to the physical light neutrino mass matrix whereas $M_\nu^{(2)}$ and $M_\nu^{(3)}$ are the heavy quasi-Dirac neutrino mass entries. Note that the physical eigenstates include three active neutrinos and six heavy, mainly isosinglet, neutrinos. The heavy quasi-Dirac neutrinos have a small splitting μ.

In the limit of vanishing contributions from linear seesaw ($v_L \ll v_R$), the light neutrino mass matrix becomes

$$M_\nu^{(1)} \approx \mu = \begin{pmatrix} r\lambda_1 & \lambda_2 e^{i\psi} & \lambda_2 e^{-i\psi} \\ \lambda_2 e^{i\psi} & \lambda_1 e^{-i\psi} & r\lambda_2 \\ \lambda_2 e^{-i\psi} & r\lambda_2 & \lambda_1 e^{i\psi} \end{pmatrix} \frac{v_\xi}{\sqrt{2+r^2}}. \tag{5.5}$$

Taking real Yukawa couplings λ_i and VEVs, $M_\nu^{(1)}$ display explicit generalized $\mu - \tau$ symmetry [40–42]

$$X^T M_\nu^{(1)} X = M_\nu^{(1)*}, \tag{5.6}$$

with

$$X = \begin{pmatrix} 1 & 0 & 0 \\ 0 & 0 & 1 \\ 0 & 1 & 0 \end{pmatrix}. \tag{5.7}$$

The most general matrix V_ν that diagonalizes $M_\nu^{(1)}$ through $V_\nu^T M_\nu^{(1)} V_\nu = \mathrm{diag}(m_1^\nu, m_2^\nu, m_3^\nu)$ is given by [43, 44]

$$V_\nu = \Sigma O_{23} O_{13} O_{12} Q_\nu, \tag{5.8}$$

where

$$\Sigma = \begin{pmatrix} 1 & 0 & 0 \\ 0 & \frac{1}{\sqrt{2}} & \frac{i}{\sqrt{2}} \\ 0 & \frac{1}{\sqrt{2}} & -\frac{i}{\sqrt{2}} \end{pmatrix}, \tag{5.9}$$

JHEP07(2017)118

is the Takagi factorization matrix of X defined as $X = \Sigma\Sigma^T$, O_{ij} are 3×3 orthogonal matrix parameterized as

$$O_{23} = \begin{pmatrix} 1 & 0 & 0 \\ 0 & \cos\omega_{23} & \sin\omega_{23} \\ 0 & -\sin\omega_{23} & \cos\omega_{23} \end{pmatrix}, \qquad O_{13} = \begin{pmatrix} \cos\omega_{13} & 0 & \sin\omega_{13} \\ 0 & 1 & 0 \\ -\sin\omega_{13} & 0 & \cos\omega_{13} \end{pmatrix},$$
$$O_{12} = \begin{pmatrix} \cos\omega_{12} & \sin\omega_{12} & 0 \\ -\sin\omega_{12} & \cos\omega_{12} & 0 \\ 0 & 0 & 1 \end{pmatrix}, \tag{5.10}$$

and $Q_\nu = \mathrm{diag}(e^{-i\pi k_1/2}, e^{-i\pi k_2/2}, e^{-i\pi k_3/2})$ is a diagonal matrix with $k_i = 0, 1, 2, 3$.

Notice that, with real Yukawa couplings λ_i and VEVs in eq. (5.4), we have a reduced number of parameters, leading to the following relations:

$$\begin{aligned} \tan 2\omega_{12} &= \frac{4\sin\omega_{13}\left[\sin\left(2\psi+\omega_{23}\right)+\sin 3\omega_{23}\right]}{\left(3\cos 2\omega_{13}-1\right)\cos\left(2\psi+\omega_{23}\right)+\left(\cos 2\omega_{13}-3\right)\cos 3\omega_{23}}\,, \\ \lambda_1 &= -\sqrt{2}\lambda_2\tan\omega_{13}\cos\left(\psi-\omega_{23}\right)\csc\left(\psi+2\omega_{23}\right) \\ r &= -\frac{\sqrt{2}\left[\sin\omega_{13}\cos\left(\psi-\omega_{23}\right)\cos\left(\psi+2\omega_{23}\right)+2\cos\omega_{13}\cot 2\omega_{13}\sin\left(\psi-\omega_{23}\right)\sin\left(\psi+2\omega_{23}\right)\right]}{\sqrt{2}\sin\omega_{13}\cos\left(\psi-\omega_{23}\right)+\cos\omega_{13}\sin\left(\psi+2\omega_{23}\right)}\,. \end{aligned} \tag{5.11}$$

On the other hand, the light charged lepton mass matrix in eq. (4.4) is diagonalized by an almost diagonal unitary matrix through $V_l^\dagger M_l^{(1)} M_l^{(1)\dagger} V_l = \mathrm{diag}(m_e^2, m_\mu^2, m_\tau^2)$. Taking real entries in $M_l^{(1)}$, at first approximation V_l is dominated by the Cabibbo angle and can be written as

$$V_l \approx \begin{pmatrix} \cos\theta_0 & \sin\theta_0 & 0 \\ -\sin\theta_0 & \cos\theta_0 & 0 \\ 0 & 0 & 1 \end{pmatrix}, \qquad \sin\theta_0 \approx \lambda. \tag{5.12}$$

In this approximation, the lepton mixing matrix is given as

$$U = V_l^\dagger V_\nu. \tag{5.13}$$

In the fully "symmetrical" presentation of the lepton mixing matrix [45, 46]

$$U = \begin{pmatrix} c_{12}c_{13} & s_{12}c_{13}e^{-i\phi_{12}} & s_{13}e^{-i\phi_{13}} \\ -s_{12}c_{23}e^{i\phi_{12}} - c_{12}s_{13}s_{23}e^{-i(\phi_{23}-\phi_{13})} & c_{12}c_{23} - s_{12}s_{13}s_{23}e^{-i(\phi_{23}+\phi_{12}-\phi_{13})} & c_{13}s_{23}e^{-i\phi_{23}} \\ s_{12}s_{23}e^{i(\phi_{23}+\phi_{12})} - c_{12}s_{13}c_{23}e^{i\phi_{13}} & -c_{12}s_{23}e^{i\phi_{23}} - s_{12}s_{13}c_{23}e^{-i(\phi_{12}-\phi_{13})} & c_{13}c_{23} \end{pmatrix}, \tag{5.14}$$

with $c_{ij} = \cos\theta_{ij}$ and $s_{ij} = \sin\theta_{ij}$, the relation between flavor mixing angles and the magnitudes of the entries of the leptonic mixing matrix is

$$\sin^2\theta_{13} = |U_{e3}|^2\,, \quad \sin^2\theta_{12} = \frac{|U_{e2}|^2}{1-|U_{e3}|^2} \quad \text{and} \quad \sin^2\theta_{23} = \frac{|U_{\mu 3}|^2}{1-|U_{e3}|^2}\,. \tag{5.15}$$

JHEP07(2017)118

The Jarlskog invariant is defined as $J_{\rm CP} = {\rm Im}\,(U^*_{11}U^*_{23}U_{13}U_{21})$, and takes the form [46]

$$J_{\rm CP} = \frac{1}{8}\sin 2\theta_{12}\,\sin 2\theta_{23}\,\sin 2\theta_{13}\,\cos\theta_{13}\,\sin(\phi_{13}-\phi_{23}-\phi_{12})\,, \tag{5.16}$$

whereas the two additional Majorana-type rephasing invariants $I_1 = {\rm Im}\left(U^2_{12}U^{*2}_{11}\right)$ and $I_2 = {\rm Im}\left(U^2_{13}U^{*2}_{11}\right)$, become

$$I_1 = \frac{1}{4}\sin^2 2\theta_{12}\cos^4\theta_{13}\sin(-2\phi_{12}) \quad \text{and} \quad I_2 = \frac{1}{4}\sin^2 2\theta_{13}\cos^2\theta_{12}\sin(-2\phi_{13})\,. \tag{5.17}$$

In terms of the model parameters, the lepton mixing angles are expressed as

$$\sin^2\theta_{13} = \frac{1}{4}\left(4\cos^2\theta_0\sin^2\omega_{13} + 2\sin^2\theta_0\cos^2\omega_{13} - \sqrt{2}\sin 2\theta_0\sin 2\omega_{13}\sin\omega_{23}\right)\,, \tag{5.18}$$

$$\begin{aligned}\sin^2\theta_{12} = {}& \left[2\sin^2\theta_0\left(\sin^2\omega_{12}\sin^2\omega_{13} + \cos^2\omega_{12}\right) + 4\cos^2\theta_0\sin^2\omega_{12}\cos^2\omega_{13}\right.\\ & \left. + \sqrt{2}\sin 2\theta_0\left(\sin^2\omega_{12}\sin 2\omega_{13}\sin\omega_{23} - \sin 2\omega_{12}\cos\omega_{13}\cos\omega_{23}\right)\right]\\ & \times\left[4 - 4\cos^2\theta_0\sin^2\omega_{13} - 2\sin^2\theta_0\cos^2\omega_{13} + \sqrt{2}\sin 2\theta_0\sin 2\omega_{13}\sin\omega_{23}\right]^{-1}\,,\end{aligned} \tag{5.19}$$

$$\sin^2\theta_{23} = 1 - \frac{2\cos^2\omega_{13}}{4 - 4\cos^2\theta_0\sin^2\omega_{13} - 2\sin^2\theta_0\cos^2\omega_{13} + \sqrt{2}\sin 2\theta_0\sin 2\omega_{13}\sin\omega_{23}}\,, \tag{5.20}$$

and our predicted correlations:

$$\cos^2\theta_{13}\cos^2\theta_{23} = \frac{1}{2}\cos^2\omega_{13}\,, \tag{5.21}$$

$$\cos 2\theta_{12}\cos^2\theta_{13} = \cos 2\omega_{12}\left(\cos^2\theta_{13} - \sin^2\theta_0\right) + \frac{1}{\sqrt{2}}\sin 2\theta_0\sin 2\omega_{12}\cos\omega_{13}\cos\omega_{23}\,. \tag{5.22}$$

On the other hand, the rephasing invariant CP violation parameter combinations are

$$\begin{aligned}J_{\rm CP} = {}& \frac{1}{64}\Big\{-\sqrt{2}\sin 2\theta_0\left[4\sin 2\omega_{13}\cos 2\omega_{12}\cos\omega_{23} + \sin 2\omega_{12}\sin\omega_{23}\left(\cos\omega_{13} + 3\cos 3\omega_{13}\right)\right]\\ & + 16\cos 2\theta_0\sin 2\omega_{12}\sin\omega_{13}\cos^2\omega_{13}\Big\}.\end{aligned} \tag{5.23}$$

$$\begin{aligned}I_1 = {}& \frac{(-1)^{k_1+k_2}}{8}\sin\theta_0\cos\omega_{13}\Big\{4\sqrt{2}\cos^3\theta_0\sin 2\omega_{12}\sin\omega_{23}\cos^2\omega_{13} - \sin^3\theta_0\sin 2\omega_{12}\sin 2\omega_{13}\\ & + 2\sin\theta_0\cos^2\theta_0\left[\sin 2\omega_{12}\sin 2\omega_{13}\left(2 - \cos 2\omega_{23}\right) - 2\sin 2\omega_{23}\cos 2\omega_{12}\cos\omega_{13}\right]\\ & + \sqrt{2}\sin^2\theta_0\cos\theta_0\left[\sin 2\omega_{12}\sin\omega_{23}\left(1 - 3\cos 2\omega_{13}\right) - 4\sin\omega_{13}\cos 2\omega_{12}\cos\omega_{23}\right]\Big\}\end{aligned} \tag{5.24}$$

$$\begin{aligned}I_2 = {}& \frac{(-1)^{k_1+k_3}}{32}\Big\{\sin 2\theta_0\Big\{\sqrt{2}\sin 2\omega_{12}\sin\omega_{23}\cos\omega_{13}\left[\cos 2\theta_0\left(3 - 5\cos 2\omega_{13}\right) + 2\cos^2\omega_{13}\right]\\ & - 4\sqrt{2}\sin 2\omega_{13}\cos\omega_{23}\left(\cos 2\theta_0\cos 2\omega_{12} + \cos^2\theta_0\right)\\ & + \sin 2\theta_0\sin 2\omega_{23}\left[2\sin^2\omega_{12} + \left(3\cos 2\omega_{12} + 1\right)\cos 2\omega_{13}\right]\Big\}\\ & - 4\sin^2 2\theta_0\sin 2\omega_{12}\sin^3\omega_{13}\cos 2\omega_{23}\\ & - 4\sin^2\theta_0\left(5\cos 2\theta_0 + 3\right)\sin 2\omega_{12}\sin\omega_{13}\cos^2\omega_{13}\Big\}\,.\end{aligned} \tag{5.25}$$

JHEP07(2017)118

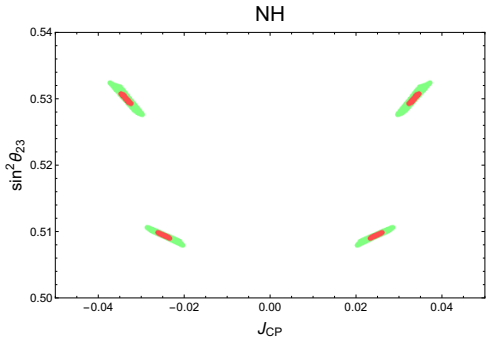

Figure 1. Predicted CP violation versus atmospheric angle for NH. Green (Red) regions correspond to 3 (1) σ values for the solar and reactor angles in eqs. (5.18), (5.19). All predicted values for $\sin^2\theta_{23}$ lie inside its 1σ region, according to the global fit [47].

Eliminating ω_{12} in the above relations using eq. (5.11), the mixing parameters depend ultimately on three angles ω_{23}, ω_{13}, ψ up to three discrete variables k_1, k_2, k_3. Furthermore, without loss of generality these angles are restricted to $\omega_{23} \in [-\pi, \pi]$, $\omega_{13} \in [-\pi/2, \pi/2]$ and $\psi \in [-\pi/2, \pi/2]$. Notice that the angle ψ in this framework is responsible for the CP violating phase in the lepton sector, since the first stage of the diagonalization process yields a real symmetric matrix

$$\Sigma^T M_\nu^{(1)} \Sigma = \frac{v_\xi}{\sqrt{2+r^2}} \begin{pmatrix} r\lambda_1 & \sqrt{2}\lambda_2 \cos\psi & -\sqrt{2}\lambda_2 \sin\psi \\ \sqrt{2}\lambda_2 \cos\psi & r\lambda_2 + \lambda_1 \cos\psi & \lambda_1 \sin\psi \\ -\sqrt{2}\lambda_2 \sin\psi & \lambda_1 \sin\psi & r\lambda_2 - \lambda_1 \cos\psi \end{pmatrix} , \tag{5.26}$$

and in the limit of vanishing ψ, this matrix is already block diagonal, implying $\omega_{23} = \omega_{13} = 0$ in eq. (5.23), which in turn leads to $J_{\rm CP} = 0$. Moreover, from eq. (5.21), notice that if $\sin^2\theta_{13}$ is allowed to vary within 3σ according to the global fit [47], then $\sin^2\theta_{23}$ is restricted to the range $(0.487, 0.539)$.

In figures 1 and 2, we give the allowed values for $\sin^2\theta_{23}$ together with the corresponding $J_{\rm CP}$ predictions in both mass orderings. For our analysis, we randomly generated parameter configurations for ω_{23}, ω_{13} and ψ corresponding to $3(1)\sigma$ values for the solar and reactor angles in eqs. (5.18), (5.19). One sees that for the Normal Hierarchy (NH) case the allowed region is severely restricted, with a fourfold degeneracy. In this case CP must necessarily be violated in oscillations, and the predicted atmospheric angle lies in the higher octant, inside its 1σ region.

In contrast, for the case of Inverted Hierarchy (IH) one sees that CP can be conserved in neutrino oscillations. Moreover, if violated, it is unlikely for CP to be maximally violated. The predicted atmospheric angle lies inside its 2σ region, preferably in the first octant.

6 Neutrinoless double beta decay

In this section we determine the effective Majorana neutrino mass parameter characterizing the neutrinoless double beta ($0\nu\beta\beta$) decay amplitude. It is given by:

$$\begin{aligned} |m_{\beta\beta}| &= \left| \sum_{i=1}^{3} m_i^\nu U_{ei}^2 \right| \\ &= \frac{1}{4} \left| m_1 \left(2\cos\theta_0 \cos\omega_{12} \cos\omega_{13} + \sqrt{2} e^{-i\omega_{23}} \sin\theta_0 \left[\sin\omega_{12} + i \sin\omega_{13} \cos\omega_{12} \right] \right)^2 \right. \end{aligned}$$

JHEP07(2017)118

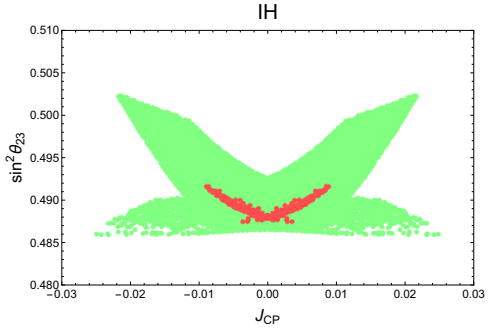

Figure 2. Predicted CP violation versus atmospheric angle for IH. Green (Red) regions correspond to 3 (1) σ values for the solar and reactor angles in eqs. (5.18), (5.19). All predicted values for $\sin^2\theta_{23}$ in this case lie into its 2σ region [47].

$$+ m_2 \left(-2\cos\theta_0 \sin\omega_{12}\cos\omega_{13} + \sqrt{2}e^{-i\omega_{23}}\sin\theta_0\left[\cos\omega_{12} - i\sin\omega_{12}\sin\omega_{13}\right]\right)^2$$
$$- m_3 \left(\sqrt{2}e^{-i\omega_{23}}\sin\theta_0\cos\omega_{13} + 2i\cos\theta_0\sin\omega_{13}\right)^2\Bigg|, \tag{6.1}$$

where U_{ei}^2 and m_{ν_i} are the lepton mixing matrix elements and the light active neutrino masses, respectively. The light active neutrino masses can be written in terms of the parameters of the model as

$$\begin{aligned}
m_1 =& \frac{\lambda_2 v_\xi}{\sqrt{2+r^2}}\Bigg\{\frac{\sqrt{2}\tan\omega_{13}\sin 2\left(\psi-\omega_{23}\right)+\left(1-4\tan^2\omega_{13}\right)\cos\left(2\psi+\omega_{23}\right)-\cos 3\omega_{23}}{2\tan\omega_{13}\left[\sqrt{2}\sin\left(\psi+2\omega_{23}\right)+2\tan\omega_{13}\cos\left(\psi-\omega_{23}\right)\right]} \\
&- \frac{\left(3\cos 2\omega_{13}-1\right)\cos\left(2\psi+\omega_{23}\right)+\left(\cos 2\omega_{13}-3\right)\cos 3\omega_{23}}{2\sqrt{2}\sin 2\omega_{13}\sin\left(\psi+2\omega_{23}\right)} \\
&\times\sqrt{1+\frac{16\sin^2\omega_{13}\left[\sin\left(2\psi+\omega_{23}\right)+\sin\left(3\omega_{23}\right)\right]^2}{\left[\left(3\cos 2\omega_{13}-1\right)\cos\left(2\psi+\omega_{23}\right)+\left(\cos 2\omega_{13}-3\right)\cos 3\omega_{23}\right]^2}}\Bigg\}, \\
m_2 =& \frac{\lambda_2 v_\xi}{\sqrt{2+r^2}}\Bigg\{\frac{\sqrt{2}\tan\omega_{13}\sin 2\left(\psi-\omega_{23}\right)+\left(1-4\tan^2\omega_{13}\right)\cos\left(2\psi+\omega_{23}\right)-\cos 3\omega_{23}}{2\tan\omega_{13}\left[\sqrt{2}\sin\left(\psi+2\omega_{23}\right)+2\tan\omega_{13}\cos\left(\psi-\omega_{23}\right)\right]} \\
&+ \frac{\left(3\cos 2\omega_{13}-1\right)\cos\left(2\psi+\omega_{23}\right)+\left(\cos 2\omega_{13}-3\right)\cos 3\omega_{23}}{2\sqrt{2}\sin 2\omega_{13}\sin\left(\psi+2\omega_{23}\right)} \\
&\times\sqrt{1+\frac{16\sin^2\omega_{13}\left[\sin\left(2\psi+\omega_{23}\right)+\sin\left(3\omega_{23}\right)\right]^2}{\left[\left(3\cos 2\omega_{13}-1\right)\cos\left(2\psi+\omega_{23}\right)+\left(\cos 2\omega_{13}-3\right)\cos 3\omega_{23}\right]^2}}\Bigg\}, \\
m_3 =& \frac{\lambda_2 v_\xi}{\sqrt{2+r^2}}\left\{\frac{\tan^2\omega_{13}\left[\cos\left(\psi+2\omega_{23}\right)+\cos 3\psi\right]\csc^2\left(\psi+2\omega_{23}\right)-\sqrt{2}\cot\omega_{13}\sin\left(\psi-\omega_{23}\right)}{1+\sqrt{2}\tan\omega_{13}\cos\left(\psi-\omega_{23}\right)\csc\left(\psi+2\omega_{23}\right)}\right\},
\end{aligned} \tag{6.2}$$

with

$$Q_\nu^T \,\mathrm{diag}(m_1, m_2, m_3) Q_\nu = \mathrm{diag}(m_1^\nu, m_2^\nu, m_3^\nu).$$

We show in figure 3 the effective Majorana neutrino mass parameter $|m_{\beta\beta}|$ versus the lightest active neutrino mass for the cases of normal and inverted neutrino mass hierarchies.

JHEP07(2017)118

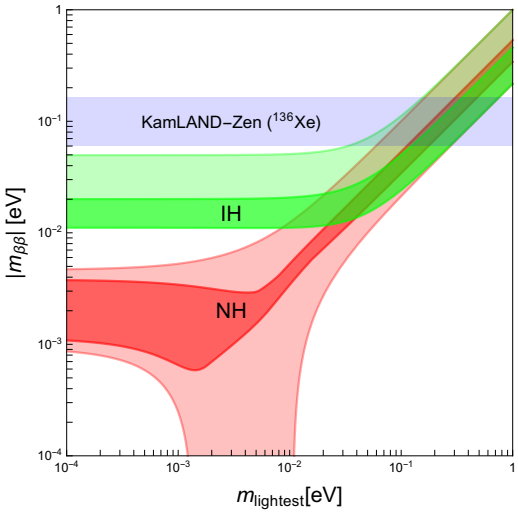

Figure 3. Effective Majorana neutrino mass parameter $|m_{\beta\beta}|$ as a function of the lightest active neutrino mass m_{lightest}. The light shaded regions indicate the 3σ ranges calculated from the oscillation parameter uncertainties [47], and the dark shaded areas correspond to the allowed values predicted by the model. The horizontal blue band indicates 90% C.L. upper limits on $|m_{\beta\beta}|$ with ^{136}Xe from the KamLAND-Zen experiment [49].

In order to determine the predicted ranges for $|m_{\beta\beta}|$ in our model, we have randomly generated the angles ω_{23}, ω_{13} and ψ, as well as the light active neutrino mass scale $m_\nu = \frac{\lambda_2 v_\xi}{\sqrt{2+r^2}}$ in a range of values where the neutrino mass squared splittings and the leptonic mixing parameters are consistent with the observed neutrino oscillation data. Our predicted range of values for the effective Majorana neutrino mass parameter has a lower bound, even in the case of normal hierarchy, indicating that a complete destructive interference among the three light neutrinos is prevented by our symmetry and the current oscillation data.

The corresponding $0\nu\beta\beta$ decay rates are within the reach of the next-generation bolometric CUORE experiment [48] or, more realistically, of the next-to-next-generation ton-scale $0\nu\beta\beta$-decay experiments. It is worth mentioning that the Majorana neutrino mass parameter has an upper bound on $|m_{\beta\beta}| \leq (61 - 165)$ meV at 90% C.L, as indicated by the KamLAND-Zen experiment from the limit on the ^{136}Xe $0\nu\beta\beta$ decay half-life $T^{0\nu\beta\beta}_{1/2}(^{136}\text{Xe}) \geq 1.07\times10^{26}$ yr [49]. This bound will be improved within a not too far future. The GERDA "phase-II"experiment [50, 51] is expected to reach $T^{0\nu\beta\beta}_{1/2}(^{76}\text{Ge}) \geq 2\times10^{26}$ yr, corresponding to $|m_{\beta\beta}| \leq 100$ meV. A bolometric CUORE experiment, using ^{130}Te [48], is currently under construction and its estimated sensitivity is close to about $T^{0\nu\beta\beta}_{1/2}(^{130}\text{Te}) \sim 10^{26}$ yr, implying $|m_{\beta\beta}| \leq 50$ meV. Furthermore, there are plans for ton-scale next-to-next generation $0\nu\beta\beta$ experiments with ^{136}Xe [52, 53] and ^{76}Ge [50, 54], asserting sensitivities over $T^{0\nu\beta\beta}_{1/2} \sim 10^{27}$ yr, corresponding to $|m_{\beta\beta}| \sim 12 - 30$ meV.

7 Discussions and conclusions

We have proposed a realistic extension of the standard model within the Pati-Salam framework. The theory incorporates a flavor symmetry based on the $\Delta\,(27)$ group and realizes a

JHEP07(2017)118

realistic Froggatt-Nielsen picture of quark mixing. Concerning the lepton sector, neutrino masses arise from an inverse seesaw mechanism and the allowed ranges for the atmospheric mixing angle θ_{23} and CP violating phase δ_{CP} are rather restricted once one takes into account the precise measurements of the remaining oscillation parameters. This makes the model rather predictive. Our main neutrino oscillation results are summarized in figures 1 and 2. We find that, for normal neutrino mass ordering, the atmospheric angle must lie in the higher octant and that CP must be violated in oscillations. In contrast, for inverse hierarchy, the lower octant is favored and the range of allowed Jarlskog invariant extends from zero up to a non-maximal value. Our results concerning $0\nu\beta\beta$ decay are summarized in figure 3. They indicate the existence of a lower bound for the $0\nu\beta\beta$ decay rate, a feature also encountered in other flavor models [55–59]. As mentioned, neutrino masses arise from a low-scale seesaw mechanism, whose messengers may be produced at the LHC either through a charged or neutral gauge portal [14, 16, 60]. Admittedly, the model is rather complex, especially in its scalar sector. However, it serves as a "proof-of-concept" attempt, namely, to our knowledge this is the first time that a fully realistic and to some extent predictive flavor realization of a Pati-Salam scenario is given.

Acknowledgments

This research is supported by the Spanish grants FPA2014-58183-P, Multidark CSD2009-00064, SEV-2014-0398 (MINECO) and PROMETEOII/2014/084 (Generalitat Valenciana); Chilean grants Fondecyt No. 1170803, No. 1150792 and CONICYT PIA/Basal FB0821 and ACT1406; and Mexican grant CONACYT No. 274397. A.E.C.H is very grateful to Professor Hoang Ngoc Long and the other members of its group for the warm hospitality of the Institute of Physics, Vietnam Academy of Science and Technology, where this work was completed.

A Product rules of the $\Delta(27)$ discrete group

The $\Delta(27)$ discrete group is a subgroup of SU(3), has 27 elements divided into 11 conjugacy classes, so that it has 11 irreducible representations. These irreducible representations are: two triplets, i.e., $\mathbf{3}_{[0][1]}$ (which we denote by $\mathbf{3}$) and its conjugate $\mathbf{3}_{[0][2]}$ (which we denote by $\overline{\mathbf{3}}$) and 9 singlets, i.e., $\mathbf{1}_{k,l}$ $(k,l=0,1,2)$, where k and l correspond to the Z_3 and Z_3' charges, respectively [4]. The $\Delta(27)$ discrete group is a simple group of the type $\Delta(3n^2)$ with $n=3$ and is isomorphic to the semi-direct product group $(Z_3'\times Z_3'')\rtimes Z_3$ [4]. Indeed, the simplest group of the type $\Delta(3n^2)$ is $\Delta(3)\equiv Z_3$. The next group is $\Delta(12)$, which is isomorphic to A_4. Thus, the $\Delta(27)$ discrete group is the next simplest nontrivial group of the type $\Delta(3n^2)$. It is worth mentioning that one can write any element of the $\Delta(27)$ discrete group as $b^k a^m a'^n$, where b, a and a' correspond to the generators of the Z_3, Z_3' and Z_3'' cyclic groups, respectively. These generators fulfill the relations:

$$\begin{aligned} a^3 = a'^3 = b^3 = 1, \qquad & aa' = a'a, \\ bab^{-1} = a^{-1}a'^{-1}, \qquad & ba'b^{-1} = a, \end{aligned} \tag{A.1}$$

JHEP07(2017)118

	h	$\chi 1_{(r,s)}$	$\chi 3_{[0,1]}$	$\chi 3_{[0,2]}$
$1C_1$	1	1	3	3
$1C_1^{(1)}$	1	1	$3\omega^2$	3ω
$1C_1^{(2)}$	1	1	3ω	$3\omega^2$
$3C_1^{(0,1)}$	3	ω^s	0	0
$3C_1^{(0,2)}$	3	ω^{2s}	0	0
$C_3^{(1,p)}$	3	ω^{r+sp}	0	0
$C_3^{(2,p)}$	3	ω^{2r+sp}	0	0

Table 5. Characters of $\Delta(27)$

The characters of the $\Delta(27)$ discrete group are shown in table 5. Here n is the number of elements, h is the order of each element, and $\omega = e^{\frac{2\pi i}{3}} = -\frac{1}{2} + i\frac{\sqrt{3}}{2}$ is the cube root of unity, which satisfies the relations $1 + \omega + \omega^2 = 0$ and $\omega^3 = 1$. The conjugacy classes of $\Delta(27)$ are given by:

$$\begin{aligned}
C_1 &: \quad \{e\}, && h = 1,\\
C_1^{(1)} &: \quad \{a, a'^2\}, && h = 3,\\
C_1^{(2)} &: \quad \{a^2, a'\}, && h = 3,\\
C_3^{(0,1)} &: \quad \{a'^2 a'^2\}, && h = 3,\\
C_3^{(0,2)} &: \quad \{a'^2, a^2, aa'\}, && h = 3,\\
C_3^{(1,p)} &: \{ba^p, ba^{p-1}a'^{p-2}a'^2\}, && h = 3,\\
C_3^{(2,p)} &: \{ba^p, ba^{p-1}a'^{p-2}a'^2\}, && h = 3.
\end{aligned}$$

The tensor products between $\Delta(27)$ triplets are described by the following relations [4]:

$$\begin{aligned}
\begin{pmatrix} x_{1,-1} \\ x_{0,1} \\ x_{-1,0} \end{pmatrix}_{\mathbf{3}} \otimes \begin{pmatrix} y_{1,-1} \\ y_{0,1} \\ y_{-1,0} \end{pmatrix}_{\mathbf{3}} &= \begin{pmatrix} x_{1,-1}y_{1,-1} \\ x_{0,1}y_{0,1} \\ x_{-1,0}y_{-1,0} \end{pmatrix}_{\bar{\mathbf{3}}_{S_1}} \oplus \frac{1}{2}\begin{pmatrix} x_{0,1}y_{-1,0} + x_{-1,0}y_{0,1} \\ x_{-1,0}y_{1,-1} + x_{1,-1}y_{-1,0} \\ x_{1,-1}y_{0,1} + x_{0,1}y_{1,-1} \end{pmatrix}_{\bar{\mathbf{3}}_{S_2}} \\
&\oplus \frac{1}{2}\begin{pmatrix} x_{0,1}y_{-1,0} - x_{-1,0}y_{0,1} \\ x_{-1,0}y_{1,-1} - x_{1,-1}y_{-1,0} \\ x_{1,-1}y_{0,1} - x_{0,1}y_{1,-1} \end{pmatrix}_{\bar{\mathbf{3}}_A},
\end{aligned} \tag{A.2}$$

$$\begin{aligned}
\begin{pmatrix} x_{2,-2} \\ x_{0,2} \\ x_{-2,0} \end{pmatrix}_{\bar{\mathbf{3}}} \otimes \begin{pmatrix} y_{2,-2} \\ y_{0,2} \\ y_{-2,0} \end{pmatrix}_{\bar{\mathbf{3}}} &= \begin{pmatrix} x_{2,-2}y_{2,-2} \\ x_{0,2}y_{0,2} \\ x_{-2,0}y_{-2,0} \end{pmatrix}_{\mathbf{3}_{S_1}} \oplus \frac{1}{2}\begin{pmatrix} x_{0,2}y_{-2,0} + x_{-2,0}y_{0,2} \\ x_{-2,0}y_{2,-2} + x_{2,-2}y_{-2,0} \\ x_{2,-2}y_{0,2} + x_{0,2}y_{2,-2} \end{pmatrix}_{\mathbf{3}_{S_2}} \\
&\oplus \frac{1}{2}\begin{pmatrix} x_{0,2}y_{-2,0} - x_{-2,0}y_{0,2} \\ x_{-2,0}y_{2,-2} - x_{2,-2}y_{-2,0} \\ x_{2,-2}y_{0,2} - x_{0,2}y_{2,-2} \end{pmatrix}_{\mathbf{3}_A},
\end{aligned} \tag{A.3}$$

$$\begin{pmatrix} x_{1,-1} \\ x_{0,1} \\ x_{-1,0} \end{pmatrix}_{\mathbf{3}} \otimes \begin{pmatrix} y_{-1,1} \\ y_{0,-1} \\ y_{1,0} \end{pmatrix}_{\bar{\mathbf{3}}} = \sum_r (x_{1,-1}y_{-1,1} + \omega^{2r}x_{0,1}y_{0,-1} + \omega^r x_{-1,0}y_{1,0})_{\mathbf{1}_{(r,0)}}$$

JHEP07(2017)118

Singlets	$\mathbf{1}_{01}$	$\mathbf{1}_{02}$	$\mathbf{1}_{10}$	$\mathbf{1}_{11}$	$\mathbf{1}_{12}$	$\mathbf{1}_{20}$	$\mathbf{1}_{21}$	$\mathbf{1}_{22}$
$\mathbf{1}_{01}$	$\mathbf{1}_{02}$	$\mathbf{1}_{00}$	$\mathbf{1}_{11}$	$\mathbf{1}_{12}$	$\mathbf{1}_{10}$	$\mathbf{1}_{21}$	$\mathbf{1}_{22}$	$\mathbf{1}_{20}$
$\mathbf{1}_{02}$	$\mathbf{1}_{00}$	$\mathbf{1}_{01}$	$\mathbf{1}_{12}$	$\mathbf{1}_{10}$	$\mathbf{1}_{11}$	$\mathbf{1}_{22}$	$\mathbf{1}_{20}$	$\mathbf{1}_{21}$
$\mathbf{1}_{10}$	$\mathbf{1}_{11}$	$\mathbf{1}_{12}$	$\mathbf{1}_{20}$	$\mathbf{1}_{21}$	$\mathbf{1}_{22}$	$\mathbf{1}_{00}$	$\mathbf{1}_{01}$	$\mathbf{1}_{02}$
$\mathbf{1}_{11}$	$\mathbf{1}_{12}$	$\mathbf{1}_{10}$	$\mathbf{1}_{21}$	$\mathbf{1}_{22}$	$\mathbf{1}_{20}$	$\mathbf{1}_{01}$	$\mathbf{1}_{02}$	$\mathbf{1}_{00}$
$\mathbf{1}_{12}$	$\mathbf{1}_{10}$	$\mathbf{1}_{11}$	$\mathbf{1}_{22}$	$\mathbf{1}_{20}$	$\mathbf{1}_{21}$	$\mathbf{1}_{02}$	$\mathbf{1}_{00}$	$\mathbf{1}_{01}$
$\mathbf{1}_{20}$	$\mathbf{1}_{21}$	$\mathbf{1}_{22}$	$\mathbf{1}_{00}$	$\mathbf{1}_{01}$	$\mathbf{1}_{02}$	$\mathbf{1}_{10}$	$\mathbf{1}_{11}$	$\mathbf{1}_{12}$
$\mathbf{1}_{21}$	$\mathbf{1}_{22}$	$\mathbf{1}_{20}$	$\mathbf{1}_{01}$	$\mathbf{1}_{02}$	$\mathbf{1}_{00}$	$\mathbf{1}_{11}$	$\mathbf{1}_{12}$	$\mathbf{1}_{10}$
$\mathbf{1}_{22}$	$\mathbf{1}_{20}$	$\mathbf{1}_{21}$	$\mathbf{1}_{02}$	$\mathbf{1}_{00}$	$\mathbf{1}_{01}$	$\mathbf{1}_{12}$	$\mathbf{1}_{10}$	$\mathbf{1}_{11}$

Table 6. The singlet multiplications of the group $\Delta(27)$.

$$\oplus \sum_r (x_{1,-1}y_{0,-1} + \omega^{2r} x_{0,1}y_{1,0} + \omega^r x_{-1,0}y_{-1,1})_{\mathbf{1}_{(r,1)}}$$
$$\oplus \sum_r (x_{1,-1}y_{1,0} + \omega^{2r} x_{0,1}y_{-1,1} + \omega^r x_{-1,0}y_{0,-1})_{\mathbf{1}_{(r,2)}}, \tag{A.4}$$

where we introduced the shorthand notation $\mathbf{3}_{[0][1]} \equiv \mathbf{3}$ and $\mathbf{3}_{[0][2]} \equiv \bar{\mathbf{3}}$ used in eq. (2.8). In the above formulas $\mathbf{3}_A$ and $\mathbf{3}_{S_{1,2}}$ are an antisymmetric and two variants of symmetric triplets. The multiplication rules between $\Delta(27)$ singlets and $\Delta(27)$ triplets are given by [4]:

$$\begin{pmatrix} x_{(1,-1)} \\ x_{(0,1)} \\ x_{(-1,0)} \end{pmatrix}_{\mathbf{3}_{[0][1]}} \otimes (z)_{1_{k,l}} = \begin{pmatrix} x_{(1,-1)}z \\ \omega^r x_{(0,1)}z \\ \omega^{2r} x_{(-1,0)}z \end{pmatrix}_{\mathbf{3}_{[l][1+l]}}, \tag{A.5}$$

$$\begin{pmatrix} x_{(2,-2)} \\ x_{(0,2)} \\ x_{(-2,0)} \end{pmatrix}_{\mathbf{3}_{[0][2]}} \otimes (z)_{1_{k,l}} = \begin{pmatrix} x_{(2,-2)}z \\ \omega^r x_{(0,2)}z \\ \omega^{2r} x_{(-2,0)} \end{pmatrix}_{\mathbf{3}_{[l][2+l]}}. \tag{A.6}$$

The tensor products of $\Delta(27)$ singlets $\mathbf{1}_{k,\ell}$ and $\mathbf{1}_{k',\ell'}$ take the form [4]:

$$\mathbf{1}_{k,\ell} \otimes \mathbf{1}_{k',\ell'} = \mathbf{1}_{k+k' \bmod 3, \ell+\ell' \bmod 3}. \tag{A.7}$$

From the equation given above, we obtain explicitly the singlet multiplication rules of the $\Delta(27)$ group, which are given in table 6.

B Scalar potential for one $\Delta(27)$ scalar triplet

The scalar potential for a $\Delta(27)$ scalar triplet, i.e., ξ is given by:

$$\begin{aligned} V = & -\mu_\xi^2 (\xi\xi^*)_{\mathbf{1_{0,0}}} + \kappa_1 (\xi\xi^*)_{\mathbf{1_{0,0}}} (\xi\xi^*)_{\mathbf{1_{0,0}}} + \kappa_2 (\xi\xi^*)_{\mathbf{1_{1,0}}} (\xi\xi^*)_{\mathbf{1_{2,0}}} + \kappa_3 (\xi\xi^*)_{\mathbf{1_{0,1}}} (\xi\xi^*)_{\mathbf{1_{0,2}}} \\ & + \kappa_4 \left[(\xi\xi^*)_{\mathbf{1_{1,1}}} (\xi\xi^*)_{\mathbf{1_{2,2}}} + \text{h.c.} \right] + \kappa_5 (\xi\xi)_{\bar{\mathbf{3}}_{\mathbf{S_1}}} (\xi^*\xi^*)_{\mathbf{3}_{S_1}} + \kappa_6 (\xi\xi)_{\bar{\mathbf{3}}_{\mathbf{S_2}}} (\xi^*\xi^*)_{\mathbf{3}_{S_2}} \\ & + \kappa_7 \left[(\xi\xi)_{\bar{\mathbf{3}}_{\mathbf{S_1}}} (\xi^*\xi^*)_{\mathbf{3}_{S_2}} + \text{h.c.} \right] \end{aligned} \tag{B.1}$$

JHEP07(2017)118

Assuming the VEV configuration for the $\Delta(27)$ scalar triplet ξ:

$$\langle \xi \rangle = \frac{v_\xi}{\sqrt{2+r^2}} \left(r, e^{-i\psi}, e^{i\psi} \right), \tag{B.2}$$

We find that the scalar potential minimization equations are:

$$\begin{aligned}
\frac{\partial V}{\partial \xi_1} &= \frac{2v_\xi^3 \left\{ (2\kappa_3 + \kappa_4 + 2\kappa_7)\cos\psi + r\left[2\kappa_3 + \kappa_4 + 2\kappa_7 + 2(\kappa_1 + \kappa_2 + \kappa_5) r^2\right]\right\}}{(r^2+2)^{3/2}} \\
&\quad + \frac{2v_\xi \left[2(2\kappa_1 - \kappa_2 + \kappa_3 - \kappa_4 + \kappa_6) r v_\xi^2 \cos 2\psi - \mu_\xi^2 r \left(r^2+2\right)\right]}{(r^2+2)^{3/2}} \\
&= 0 \\
\frac{\partial V}{\partial \xi_2} &= \frac{e^{-3i\psi} v_\xi^3 \left[4(\kappa_1 + \kappa_2 + \kappa_5) + 2(2\kappa_1 - \kappa_2 + \kappa_3 - \kappa_4 + \kappa_6) r^2 e^{2i\psi}\right]}{(r^2+2)^{3/2}} \\
&\quad + \frac{e^{i\psi} v_\xi^3 \left[4\kappa_1 - 2\kappa_2 + 2\kappa_6 + 2\kappa_7 r^2 + 2\kappa_3 \left(r^2+1\right) + \kappa_4 \left(r^2-2\right)\right]}{(r^2+2)^{3/2}} \\
&\quad + \frac{e^{-3i\psi} \left\{ v_\xi^3 \left[2(2\kappa_3 + \kappa_4 + 2\kappa_7) r e^{3i\psi} + (2\kappa_3 + \kappa_4 + 2\kappa_7) r e^{5i\psi}\right] - 2\mu_\xi^2 \left(r^2+2\right) e^{2i\psi} v_\xi \right\}}{(r^2+2)^{3/2}} \\
&= 0, \\
\frac{\partial V}{\partial \xi_3} &= \frac{e^{-2i\psi} v_\xi^3 \left[4(\kappa_1 + \kappa_2 + \kappa_5) e^{5i\psi} + 2(2\kappa_1 - \kappa_2 + \kappa_3 - \kappa_4 + \kappa_6) r^2 e^{3i\psi}\right]}{(r^2+2)^{3/2}} \\
&\quad + \frac{e^{-2i\psi} v_\xi^3 \left[e^{i\psi} \left(4\kappa_1 - 2\kappa_2 + 2\kappa_6 + 2\kappa_7 r^2 + 2\kappa_3 \left(r^2+1\right) + \kappa_4 \left(r^2-2\right)\right)\right]}{(r^2+2)^{3/2}} \\
&\quad + \frac{e^{-2i\psi} \left\{ v_\xi^3 \left[2(2\kappa_3 + \kappa_4 + 2\kappa_7) r e^{2i\psi} + (2\kappa_3 + \kappa_4 + 2\kappa_7) r\right] - 2\mu_\xi^2 \left(r^2+2\right) e^{3i\psi} v_\xi \right\}}{(r^2+2)^{3/2}} \\
&= 0.
\end{aligned} \tag{B.3}$$

Then, from the scalar potential minimization equations, we find the following relations:

$$\begin{aligned}
\mu_\xi^2 &= \frac{v_\xi^2}{r\left(r^2+2\right)} \Big\{ (2\kappa_3 + \kappa_4 + 2\kappa_7)\cos\psi + r\left[2\kappa_3 + \kappa_4 + 2\kappa_7 + 2(\kappa_1 + \kappa_2 + \kappa_5) r^2\right] \\
&\quad + 2(2\kappa_1 - \kappa_2 + \kappa_3 - \kappa_4 + \kappa_6) r \cos 2\psi \Big\}, \\
&\quad 2\left[-6\kappa_2 - 4\kappa_5 + 2\kappa_6 + 2\kappa_7 r^2 + 2\kappa_3 \left(r^2+1\right) + \kappa_4 \left(r^2-2\right)\right] \sin\psi \cos\psi \\
&\quad + \left[2(2\kappa_3 + \kappa_4 + 2\kappa_7) r \cos 2\psi + 3(2\kappa_3 + \kappa_4 + 2\kappa_7) r\right] \sin\psi = 0, \\
&\quad (2\kappa_3 + \kappa_4 + 2\kappa_7)\left(r^2 - 1\right)\cos 2\psi \\
&\quad - r\left\{ 2(2\kappa_3 + \kappa_4 + 2\kappa_7) + \left[6\kappa_2 - 4\kappa_3 + \kappa_4 + 4\kappa_5 - 2(\kappa_6 + \kappa_7)\right] r^2 \right\} \cos\psi \\
&\quad + (2\kappa_3 + \kappa_4 + 2\kappa_7)\left(2r^2 - 1\right) + 2(3\kappa_2 - \kappa_3 + \kappa_4 + 2\kappa_5 - \kappa_6) r \cos 3\psi = 0.
\end{aligned} \tag{B.4}$$

Thus, the VEV pattern for the $\Delta(27)$ triplet, i.e., ξ given by eq. (B.2), is compatible with a global minimum of the scalar potential of eq. (B.1) for a large region of parameter space.

JHEP07(2017)118

C Scalar potential for three $\Delta(27)$ scalar triplets

The scalar potential for the three $\Delta(27)$ scalar triplets ρ, τ and η is

$$V = V_\rho + V_\tau + V_\eta + V_{\rho,\tau} + V_{\tau,\eta} + V_{\rho,\eta}\,, \tag{C.1}$$

where V_ρ, V_τ and V_η are the scalar potentials for the $\Delta(27)$ scalar triplets ρ, τ and η, respectively, whereas $V_{\rho,\tau}$, $V_{\tau,\eta}$ and $V_{\rho,\eta}$ describe interaction terms involving the pairs (ρ, τ), (τ, η) and (ρ, η). The different parts of the scalar potential for the three $\Delta(27)$ scalar triplets take the form:

$$\begin{aligned}
V_\rho =& -\mu_\rho^2 \left(\rho\rho^*\right)_{\mathbf{1_{0,0}}} + \kappa_{\rho,1} \left(\rho\rho^*\right)_{\mathbf{1_{0,0}}} \left(\rho\rho^*\right)_{\mathbf{1_{0,0}}} + \kappa_{\rho,2} \left(\rho\rho^*\right)_{\mathbf{1_{1,0}}} \left(\rho\rho^*\right)_{\mathbf{1_{2,0}}} \\
&+\kappa_{\rho,3} \left(\rho\rho^*\right)_{\mathbf{1_{0,1}}} \left(\rho\rho^*\right)_{\mathbf{1_{0,2}}} + \kappa_{\rho,4} \left[\left(\rho\rho^*\right)_{\mathbf{1_{1,1}}} \left(\rho\rho^*\right)_{\mathbf{1_{2,2}}} + \text{h.c.}\right] + \kappa_{\rho,5} \left(\rho\rho\right)_{\mathbf{\overline{3}_{S_1}}} \left(\rho^*\rho^*\right)_{\mathbf{3}_{S_1}} \\
&+\kappa_{\rho,6} \left(\rho\rho\right)_{\mathbf{\overline{3}_{S_2}}} \left(\rho^*\rho^*\right)_{\mathbf{3}_{S_2}} + \kappa_{\rho,7} \left[\left(\rho\rho\right)_{\mathbf{\overline{3}_{S_1}}} \left(\rho^*\rho^*\right)_{\mathbf{3}_{S_2}} + \text{h.c.}\right]\,, \qquad \text{(C.2)} \\
V_\tau =& \; V_\rho \left(\rho \to \tau, \mu_\rho \to \mu_\tau, \kappa_{\rho,j} \to \kappa_{\tau,j}\right)\,, \qquad \text{(C.3)} \\
V_\eta =& \; V_\rho \left(\rho \to \eta, \mu_\rho \to \mu_\eta, \kappa_{\rho,j} \to \kappa_{\eta,j}\right)\,, \qquad \text{(C.4)} \\
V_{\rho,\tau} =& \; \gamma_{\rho\tau,1} \left(\rho\rho^*\right)_{\mathbf{1_{0,0}}} \left(\tau\tau^*\right)_{\mathbf{1_{0,0}}} + \kappa_{\rho\tau,1} \left(\rho\tau^*\right)_{\mathbf{1_{0,0}}} \left(\rho^*\tau\right)_{\mathbf{1_{0,0}}} + \gamma_{\rho\tau,2} \left[\left(\rho\rho^*\right)_{\mathbf{1_{1,0}}} \left(\tau\tau^*\right)_{\mathbf{1_{2,0}}} + \text{h.c.}\right] \\
&+\kappa_{\rho\tau,2} \left[\left(\rho\tau^*\right)_{\mathbf{1_{1,0}}} \left(\rho\tau^*\right)_{\mathbf{1_{2,0}}} + \text{h.c.}\right] + \gamma_{\rho\tau,3} \left[\left(\rho\rho^*\right)_{\mathbf{1_{0,1}}} \left(\tau\tau^*\right)_{\mathbf{1_{0,2}}} + \text{h.c.}\right] \\
&+\kappa_{\rho\tau,3} \left[\left(\rho\tau^*\right)_{\mathbf{1_{0,1}}} \left(\rho\tau^*\right)_{\mathbf{1_{0,2}}} + \text{h.c.}\right] + \gamma_{\rho\tau,4} \left[\left(\rho\rho^*\right)_{\mathbf{1_{1,1}}} \left(\tau\tau^*\right)_{\mathbf{1_{2,2}}} + \text{h.c.}\right] \\
&+\kappa_{\rho\tau,4} \left[\left(\rho\tau^*\right)_{\mathbf{1_{1,1}}} \left(\rho\tau^*\right)_{\mathbf{1_{2,2}}} + \text{h.c.}\right] + \gamma_{\rho\tau,5} \left[\left(\rho\rho\right)_{\mathbf{\overline{3}_{S_1}}} \left(\tau^*\tau^*\right)_{\mathbf{3}_{S_1}} + \text{h.c.}\right] \\
&+\gamma_{\rho\tau,6} \left[\left(\rho\rho\right)_{\mathbf{\overline{3}_{S_2}}} \left(\tau^*\tau^*\right)_{\mathbf{3}_{S_2}} + \text{h.c.}\right] + \kappa_{\rho\tau,5} \left(\rho\tau\right)_{\mathbf{\overline{3}_{S_1}}} \left(\rho^*\tau^*\right)_{\mathbf{3}_{S_1}} + \kappa_{\rho\tau,6} \left(\rho\tau\right)_{\mathbf{\overline{3}_{S_2}}} \left(\rho^*\tau^*\right)_{\mathbf{3}_{S_2}} \\
&+\gamma_{\rho\tau,7} \left[\left(\rho\rho\right)_{\mathbf{\overline{3}_{S_1}}} \left(\tau^*\tau^*\right)_{\mathbf{3}_{S_2}} + \text{h.c.}\right] + \kappa_{\rho\tau,7} \left[\left(\rho\tau\right)_{\mathbf{\overline{3}_{S_1}}} \left(\rho^*\tau^*\right)_{\mathbf{3}_{S_2}} + \text{h.c.}\right] \\
&+\kappa_{\rho\tau,8} \left[\left(\rho\tau\right)_{\mathbf{\overline{3}_{A}}} \left(\rho^*\tau^*\right)_{\mathbf{3}_{A}} + \text{h.c.}\right] + \kappa_{\rho\tau,9} \left[\left(\rho\tau\right)_{\mathbf{\overline{3}_{A}}} \left(\rho^*\tau^*\right)_{\mathbf{3}_{S_1}} + \text{h.c.}\right] \\
&+\kappa_{\rho\tau,10} \left[\left(\rho\tau\right)_{\mathbf{\overline{3}_{A}}} \left(\rho^*\tau^*\right)_{\mathbf{3}_{S_2}} + \text{h.c.}\right] \qquad \text{(C.5)} \\
V_{\rho,\eta} =& \; V_{\rho,\tau} \left(\tau \to \eta, \mu_\tau \to \mu_\eta, \kappa_{\tau,j} \to \kappa_{\eta,j}\right)\,, \qquad \text{(C.6)} \\
V_{\tau,\eta} =& \; V_{\rho,\eta} \left(\rho \to \tau, \mu_\rho \to \mu_\tau, \kappa_{\rho,j} \to \kappa_{\tau,j}\right)\,. \qquad \text{(C.7)}
\end{aligned}$$

Now we determine the conditions under which the VEV pattern for the $\Delta\,(27)$ scalar triplets is a solution of the scalar potential given in eq. (C.1). In view of the very large number of parameters of the scalar potential for the $\Delta\,(27)$ scalar triplets and in order to simplify the analysis, we assume universality in its trilinear and quartic couplings, i.e.

$$\begin{aligned}
\kappa_{\rho,i} &= \kappa_{\tau,i} = \kappa_{\eta,i} = \kappa_i, \qquad \gamma_{\rho\tau,i} = \gamma_{\rho\eta,i} = \gamma_{\tau\eta,i} = \gamma_i, \qquad i = 1, 2, \cdots 7. \\
\kappa_{\rho\tau,j} &= \kappa_{\rho\eta,j} = \kappa_{\tau\eta,j} = \lambda_j, \qquad j = 1, 2, \cdots 10
\end{aligned} \tag{C.8}$$

Considering the VEV alignment

$$\langle\rho\rangle = (v_\rho, 0, 0)\,, \qquad \langle\eta\rangle = (0, v_\eta, 0)\,, \qquad \langle\tau\rangle = (0, 0, v_\tau)\,, \tag{C.9}$$

JHEP07(2017)118

We find the following scalar potential minimization equations:

$$\begin{aligned}
\frac{\partial V}{\partial \rho_1} &= \frac{v_\rho}{2}\Big[-4\mu_\rho^2+8\left(\kappa_1+\kappa_2+\kappa_5\right)v_\rho^2-2\lambda_{10}\left(v_\tau^2-v_\eta^2\right) \\
&\qquad +\left(4\gamma_1-4\gamma_2+\lambda_6+2\lambda_8\right)\left(v_\tau^2+v_\eta^2\right)\Big], \\
&= 0 \\
\frac{\partial V}{\partial \rho_2} &= v_\rho v_\tau^2\left(2\lambda_3-\lambda_4\right)=0, \qquad \frac{\partial V}{\partial \rho_3} = v_\rho v_\eta^2\left(2\lambda_3-\lambda_4\right)=0, \\
\frac{\partial V}{\partial \tau_1} &= v_\tau v_\eta^2\left(2\lambda_3-\lambda_4\right)=0, \qquad \frac{\partial V}{\partial \tau_2} = 2v_\rho^2 v_\tau\left(\gamma_7+\lambda_3+\lambda_4\right)=0, \\
\frac{\partial V}{\partial \tau_3} &= \frac{v_\tau}{2}\left[-4\mu_\tau^2+8\left(\kappa_1+\kappa_2+\kappa_5\right)v_\tau^2+\left(4\gamma_1-4\gamma_2+\lambda_6+2\lambda_8-2\lambda_{10}\right)\left(v_\rho^2+v_\eta^2\right)\right] \\
&= 0. \\
\frac{\partial V}{\partial \eta_1} &= 2v_\tau^2 v_\eta\left(\gamma_7+\lambda_3+\lambda_4\right)=0, \qquad \frac{\partial V}{\partial \eta_3} = 2v_\rho^2 v_\eta\left(\gamma_7+\lambda_3+\lambda_4\right)=0, \\
\frac{\partial V}{\partial \eta_2} &= \frac{v_\eta}{2}\Big[-4\mu_\eta^2+8\left(\kappa_1+\kappa_2+\kappa_5\right)v_\eta^2+2\lambda_{10}\left(v_\rho^2-v_\tau^2\right) \\
&\qquad +\left(4\gamma_1-4\gamma_2+\lambda_6+2\lambda_8\right)\left(v_\rho^2+v_\tau^2\right)\Big] \\
&= 0.
\end{aligned} \tag{C.10}$$

Then, from the scalar potential minimization equations, we find the following relations:

$$\begin{aligned}
&\lambda_4 = 2\lambda_3, \qquad \gamma_7 = -\left(\lambda_3+\lambda_4\right), \\
&\mu_\rho^2 = 2\left(\kappa_1+\kappa_2+\kappa_5\right)v_\rho^2-\frac{1}{2}\lambda_{10}\left(v_\tau^2-v_\eta^2\right)+\frac{1}{4}\left(4\gamma_1-4\gamma_2+\lambda_6+2\lambda_8\right)\left(v_\tau^2+v_\eta^2\right), \\
&\mu_\tau^2 = 2\left(\kappa_1+\kappa_2+\kappa_5\right)v_\tau^2+\frac{1}{4}\left(4\gamma_1-4\gamma_2+\lambda_6+2\lambda_8-2\lambda_{10}\right)\left(v_\rho^2+v_\eta^2\right), \\
&\mu_\eta^2 = 2\left(\kappa_1+\kappa_2+\kappa_5\right)v_\eta^2+\frac{1}{2}\lambda_{10}\left(v_\rho^2-v_\tau^2\right)+\frac{1}{4}\left(4\gamma_1-4\gamma_2+\lambda_6+2\lambda_8\right)\left(v_\rho^2+v_\tau^2\right).
\end{aligned} \tag{C.11}$$

Consequently, the VEV patterns for the three $\Delta(27)$ triplet scalars given by eq. (C.9) are compatible with a global minimum of the scalar potential of eq. (C.1) for a large region of parameter space.

References

[1] T. Kajita, *Nobel lecture: discovery of atmospheric neutrino oscillations*, *Rev. Mod. Phys.* **88** (2016) 030501.

[2] A.B. McDonald, *Nobel lecture: the Sudbury Neutrino Observatory: observation of flavor change for solar neutrinos*, *Rev. Mod. Phys.* **88** (2016) 030502.

JHEP07(2017)118

[3] J.W. Valle and J.C. Romao, *Neutrinos in high energy and astroparticle physics*, John Wiley & Sons, U.S.A. (2015).

[4] H. Ishimori, T. Kobayashi, H. Ohki, Y. Shimizu, H. Okada and M. Tanimoto, *Non-abelian discrete symmetries in particle physics*, *Prog. Theor. Phys. Suppl.* **183** (2010) 1 [arXiv:1003.3552] [INSPIRE].

[5] S. Morisi and J.W.F. Valle, *Neutrino masses and mixing: a flavour symmetry roadmap*, *Fortsch. Phys.* **61** (2013) 466 [arXiv:1206.6678] [INSPIRE].

[6] S.F. King and C. Luhn, *Neutrino mass and mixing with discrete symmetry*, *Rept. Prog. Phys.* **76** (2013) 056201 [arXiv:1301.1340] [INSPIRE].

[7] J.C. Pati and A. Salam, *Lepton number as the fourth color*, *Phys. Rev.* **D 10** (1974) 275.

[8] R.N. Mohapatra and J.W.F. Valle, *Neutrino mass and baryon-number nonconservation in superstring models*, *Phys. Rev.* **D 34** (1986) 1642.

[9] E.K. Akhmedov, M. Lindner, E. Schnapka and J.W.F. Valle, *Left-right symmetry breaking in NJLS approach*, *Phys. Lett.* **B 368** (1996) 270 [hep-ph/9507275] [INSPIRE].

[10] E.K. Akhmedov, M. Lindner, E. Schnapka and J.W.F. Valle, *Dynamical left-right symmetry breaking*, *Phys. Rev.* **D 53** (1996) 2752 [hep-ph/9509255] [INSPIRE].

[11] M. Malinsky, J.C. Romao and J.W.F. Valle, *Novel supersymmetric* SO(10) *seesaw mechanism*, *Phys. Rev. Lett.* **95** (2005) 161801 [hep-ph/0506296] [INSPIRE].

[12] P. Fileviez Perez and M.B. Wise, *Low scale quark-lepton unification*, *Phys. Rev.* **D 88** (2013) 057703 [arXiv:1307.6213] [INSPIRE].

[13] C.D. Froggatt and H.B. Nielsen, *Hierarchy of quark masses, Cabibbo angles and CP-violation*, *Nucl. Phys.* **B 147** (1979) 277 [INSPIRE].

[14] F.F. Deppisch, N. Desai and J.W.F. Valle, *Is charged lepton flavor violation a high energy phenomenon?*, *Phys. Rev.* **D 89** (2014) 051302 [arXiv:1308.6789] [INSPIRE].

[15] J.A. Aguilar-Saavedra, F. Deppisch, O. Kittel and J.W.F. Valle, *Flavour in heavy neutrino searches at the LHC*, *Phys. Rev.* **D 85** (2012) 091301 [arXiv:1203.5998] [INSPIRE].

[16] S.P. Das, F.F. Deppisch, O. Kittel and J.W.F. Valle, *Heavy neutrinos and lepton flavour violation in left-right symmetric models at the LHC*, *Phys. Rev.* **D 86** (2012) 055006 [arXiv:1206.0256] [INSPIRE].

[17] A. Davidson and K.C. Wali, *Universal seesaw mechanism?*, *Phys. Rev. Lett.* **59** (1987) 393 [INSPIRE].

[18] G. Valencia and S. Willenbrock, *Quark-lepton unification and rare meson decays*, *Phys. Rev.* **D 50** (1994) 6843 [hep-ph/9409201] [INSPIRE].

[19] A.D. Smirnov, *Mass limits for scalar and gauge leptoquarks from* $K_L^0 \to e^\pm\mu^\pm, B_0 \to e^\mp\tau^\pm$ *decays*, *Mod. Phys. Lett.* **A 22** (2007) 2353 [arXiv:0705.0308] [INSPIRE].

[20] F. Hartmann, W. Kilian and K. Schnitter, *Multiple scales in Pati-Salam unification models*, *JHEP* **05** (2014) 064 [arXiv:1401.7891] [INSPIRE].

[21] W. Grimus and L. Lavoura, *The seesaw mechanism at arbitrary order: disentangling the small scale from the large scale*, *JHEP* **11** (2000) 042 [hep-ph/0008179] [INSPIRE].

[22] G. Bhattacharyya, I. de Medeiros Varzielas and P. Leser, *A common origin of fermion mixing and geometrical CP-violation and its test through Higgs physics at the LHC*, *Phys. Rev. Lett.* **109** (2012) 241603 [arXiv:1210.0545] [INSPIRE].

[23] F. Björkeroth, F.J. de Anda, I. de Medeiros Varzielas and S.F. King, *Towards a complete* $\Delta(27) \times$ SO(10) *SUSY GUT*, *Phys. Rev.* **D 94** (2016) 016006 [arXiv:1512.00850] [INSPIRE].

JHEP07(2017)118

[24] P. Chen, G.-J. Ding, A.D. Rojas, C.A. Vaquera-Araujo and J.W.F. Valle, *Warped flavor symmetry predictions for neutrino physics*, *JHEP* **01** (2016) 007 [arXiv:1509.06683] [INSPIRE].

[25] V.V. Vien, A.E. Cárcamo Hernández and H.N. Long, *The* $\Delta(27)$ *flavor* 3-3-1 *model with neutral leptons*, *Nucl. Phys.* **B 913** (2016) 792 [arXiv:1601.03300] [INSPIRE].

[26] A.E. Cárcamo Hernández, H.N. Long and V.V. Vien, *A* 3-3-1 *model with right-handed neutrinos based on the* $\Delta(27)$ *family symmetry*, *Eur. Phys. J.* **C 76** (2016) 242 [arXiv:1601.05062] [INSPIRE].

[27] A.E. Cárcamo Hernández and R. Martinez, *A predictive* 3-3-1 *model with* A_4 *flavor symmetry*, *Nucl. Phys.* **B 905** (2016) 337 [arXiv:1501.05937] [INSPIRE].

[28] A.E. Cárcamo Hernández and H.N. Long, *A highly predictive* A_4 *flavour* 3-3-1 *model with radiative inverse seesaw mechanism*, arXiv:1705.05246 [INSPIRE].

[29] A.E. Cárcamo Hernández, R. Martinez and F. Ochoa, *Fermion masses and mixings in the* 3-3-1 *model with right-handed neutrinos based on the* S_3 *flavor symmetry*, *Eur. Phys. J.* **C 76** (2016) 634 [arXiv:1309.6567] [INSPIRE].

[30] D. Emmanuel-Costa, C. Simoes and M. Tortola, *The minimal adjoint-*SU(5) $\times$ Z_4 *GUT model*, *JHEP* **10** (2013) 054 [arXiv:1303.5699] [INSPIRE].

[31] C. Arbeláez, A.E. Cárcamo Hernández, S. Kovalenko and I. Schmidt, *Adjoint* SU(5) *GUT model with* T_7 *flavor symmetry*, *Phys. Rev.* **D 92** (2015) 115015 [arXiv:1507.03852] [INSPIRE].

[32] A.E. Cárcamo Hernández, R. Martinez and J. Nisperuza, S_3 *discrete group as a source of the quark mass and mixing pattern in* 331 *models*, *Eur. Phys. J.* **C 75** (2015) 72 [arXiv:1401.0937] [INSPIRE].

[33] A.E. Cárcamo Hernández, I. de Medeiros Varzielas and N.A. Neill, *Novel Randall-Sundrum model with* S_3 *flavor symmetry*, *Phys. Rev.* **D 94** (2016) 033011 [arXiv:1511.07420] [INSPIRE].

[34] A.S. Joshipura and J.W.F. Valle, *Invisible Higgs decays and neutrino physics*, *Nucl. Phys.* **B 397** (1993) 105 [INSPIRE].

[35] C. Bonilla, J.C. Romão and J.W.F. Valle, *Electroweak breaking and neutrino mass: 'invisible' Higgs decays at the LHC (type-II seesaw)*, *New J. Phys.* **18** (2016) 033033 [arXiv:1511.07351] [INSPIRE].

[36] K. Bora, *Updated values of running quark and lepton masses at GUT scale in SM, 2HDM and MSSM*, *Horizon* **2** (2013) [arXiv:1206.5909] [INSPIRE].

[37] Z.-z. Xing, H. Zhang and S. Zhou, *Updated values of running quark and lepton masses*, *Phys. Rev.* **D 77** (2008) 113016 [arXiv:0712.1419] [INSPIRE].

[38] Particle Data Group collaboration, C. Patrignani et al., *Review of particle physics*, *Chin. Phys.* **C 40** (2016) 100001 [INSPIRE].

[39] LHCb collaboration, S. Bifani, *Status of new physics searches with* $b \to s\ell^+\ell^-$ *transitions @ LHCb*, arXiv:1705.02693 [INSPIRE].

[40] K.S. Babu, E. Ma and J.W.F. Valle, *Underlying* A_4 *symmetry for the neutrino mass matrix and the quark mixing matrix*, *Phys. Lett.* **B 552** (2003) 207 [hep-ph/0206292] [INSPIRE].

[41] W. Grimus and L. Lavoura, *A nonstandard CP transformation leading to maximal atmospheric neutrino mixing*, *Phys. Lett.* **B 579** (2004) 113 [hep-ph/0305309] [INSPIRE].

[42] S.F. King, A. Merle, S. Morisi, Y. Shimizu and M. Tanimoto, *Neutrino mass and mixing: from theory to experiment*, *New J. Phys.* **16** (2014) 045018 [arXiv:1402.4271] [INSPIRE].

JHEP07(2017)118

[43] P. Chen, G.-J. Ding, F. Gonzalez-Canales and J.W.F. Valle, *Generalized μ-τ reflection symmetry and leptonic CP-violation*, *Phys. Lett.* **B 753** (2016) 644 [arXiv:1512.01551] [INSPIRE].

[44] P. Chen, G.-J. Ding, F. Gonzalez-Canales and J.W.F. Valle, *Classifying CP transformations according to their texture zeros: theory and implications*, *Phys. Rev.* **D 94** (2016) 033002 [arXiv:1604.03510] [INSPIRE].

[45] J. Schechter and J.W.F. Valle, *Neutrino masses in* SU(2) $\times$ U(1) *theories*, *Phys.Rev.* **D 22** (1980) 2227.

[46] W. Rodejohann and J.W.F. Valle, *Symmetrical parametrizations of the lepton mixing matrix*, *Phys. Rev.* **D 84** (2011) 073011 [arXiv:1108.3484] [INSPIRE].

[47] D.V. Forero, M. Tortola and J.W.F. Valle, *Neutrino oscillations refitted*, *Phys. Rev.* **D 90** (2014) 093006 [arXiv:1405.7540] [INSPIRE].

[48] CUORE collaboration, F. Alessandria et al., *Sensitivity of CUORE to neutrinoless double-beta decay*, arXiv:1109.0494 [INSPIRE].

[49] KamLAND-Zen collaboration, A. Gando et al., *Search for Majorana neutrinos near the inverted Mass hierarchy region with KamLAND-Zen*, *Phys. Rev. Lett.* **117** (2016) 082503 [arXiv:1605.02889] [INSPIRE].

[50] I. Abt et al., *A new ^{76}Ge double beta decay experiment at LNGS: letter of intent*, hep-ex/0404039 [INSPIRE].

[51] GERDA collaboration, K.H. Ackermann et al., *The GERDA experiment for the search of $0\nu\beta\beta$ decay in ^{76}Ge*, *Eur. Phys. J.* **C 73** (2013) 2330 [arXiv:1212.4067] [INSPIRE].

[52] KamLAND-Zen collaboration, A. Gando et al., *Measurement of the double-β decay half-life of ^{136}Xe with the KamLAND-Zen experiment*, *Phys. Rev.* **C 85** (2012) 045504 [arXiv:1201.4664] [INSPIRE].

[53] EXO-200 collaboration, J.B. Albert et al., *Search for Majoron-emitting modes of double-beta decay of ^{136}Xe with EXO-200*, *Phys. Rev.* **D 90** (2014) 092004 [arXiv:1409.6829] [INSPIRE].

[54] Majorana collaboration, C.E. Aalseth et al., *The Majorana experiment*, *Nucl. Phys. Proc. Suppl.* **217** (2011) 44 [arXiv:1101.0119] [INSPIRE].

[55] L. Dorame, D. Meloni, S. Morisi, E. Peinado and J.W.F. Valle, *Constraining neutrinoless double beta decay*, *Nucl. Phys.* **B 861** (2012) 259 [arXiv:1111.5614] [INSPIRE].

[56] L. Dorame, S. Morisi, E. Peinado, J.W.F. Valle and A.D. Rojas, *A new neutrino mass sum rule from inverse seesaw*, *Phys. Rev.* **D 86** (2012) 056001 [arXiv:1203.0155] [INSPIRE].

[57] S.F. King, S. Morisi, E. Peinado and J.W.F. Valle, *Quark-lepton mass relation in a realistic A_4 extension of the standard model*, *Phys. Lett.* **B 724** (2013) 68 [arXiv:1301.7065] [INSPIRE].

[58] C. Bonilla, S. Morisi, E. Peinado and J.W.F. Valle, *Relating quarks and leptons with the T_7 flavour group*, *Phys. Lett.* **B 742** (2015) 99 [arXiv:1411.4883] [INSPIRE].

[59] J. Gehrlein, A. Merle and M. Spinrath, *Predictivity of neutrino mass sum rules*, *Phys. Rev.* **D 94** (2016) 093003 [arXiv:1606.04965] [INSPIRE].

[60] F.S. Queiroz, C. Siqueira and J.W.F. Valle, *Constraining flavor changing interactions from LHC Run-2 dilepton bounds with vector mediators*, *Phys. Lett.* **B 763** (2016) 269 [arXiv:1608.07295] [INSPIRE].

JHEP07(2017)118